**American Journal of Geophysics, Geochemistry and Geosystems**
Vol. 7, No. 1, 2021, pp. 1-21
http://www.aiscience.org/journal/aj3g
ISSN: 2381-7143 (Print); ISSN: 2381-7151 (Online)

# Prediction of Short-Term Morphological Change in Rapti River System Using ARIMA Model and Multi-Temporal Landsat Satellite Imageries

**Kuldeep Pareta*, Debashish Goswami**

Water Resource Department, DHI (India) Water & Environment Pvt. Ltd., New Delhi, India

## Abstract

In this paper, a new stochastic method has been presented for prediction of short-term morphological change, and bankline system using ARIMA model and multi-temporal Landsat satellite imageries in the meandering river. Multi-temporal satellite remote sensing data i.e. Landsat series imageries from 2006 to 2019 has been used for time-series analysis through ARIMA model. We have identified 105 morphological active vulnerable sites through multi-criteria analysis (MCA), and we have developed the short-term morphological change, and bankline shifting prediction model for these 105 vulnerable sites. We have analysed the erosion / deposition pattern, river migration, sinuosity ratio, soil characterise, soil texture, bank material, and water discharge data for these vulnerable sites. We have also developed an equation for generation of predicted points (x, y) in GIS. Statistical analysis of river bankline shifting rate at each vulnerable site (2006 to 2019) has been carried out and that was compared with river bank soil type, and sinuosity ratio. Sandy soil has the highest river bankline shifting rate and sinuosity ratio and clay and clay loam soil have the lowest river bankline shifting rate and sinuosity ratio. As we have developed that model based on banklines from Landsat imageries. We are recommending that the high-resolution satellite images i.e. QuickBird, GeoEye, WorldView to be used for digitization of banklines, subsequent this model will give more accurate result.

## Keywords

Morphological Change, Prediction Model, ARIMA Model, Landsat Satellite Imagery, Rapti River

Received: December 4, 2019 / Accepted: February 3, 2020 / Published online: January 22, 2021



## 1. Introduction

Rapti River originated in Nepal and flowing through Nepal and India is a meandering river. This is a highly dynamic river system that involves complex processes of morphological changes. Developing a simulation model to predict the meander migration and morphological changes has been a major research goal for the last decades. The river morphology is changing under varying environmental conditions at both spatial and temporal scales due to river erosion and drift through natural and anthropogenic inputs [1-3]. Processes governing river morphology include bankfull discharge, channel dynamics, runoff events, vegetation cover, and sediment supply. Channel migration and its response to altering conservational situations are extremely dependent on local aspects such as channel type, hydrological and vegetative conditions, and that are affected by anthropogenic disturbances [4]. Understanding the characterization of processes to move the channel and assess the morphological changes of the river have long been of interest to geomorphologists, geologists and engineers [5-6]. Currently, there is increased interest on this topic among geomorphologists for the study of river valleys and watershed hydrology [7]. Substantial progress has been made in understanding the channel morphology and river migration. The study of channel morphology is necessary to evaluate

* Corresponding author
E-mail address: kpareta13@gmail.com (K. Pareta), kupa@dhigroup.com (K. Pareta)

natural and human effects on morphological parameters and channel dynamics [8-10].

Predictions of channel reactions are a complex task, as these events are effectively responses to changes in the river bed. Most channel morphology studies have been focussing on deterministic models; but the river system is of a dynamic and stochastic nature. Mathematical models i.e. Autoregressive Integrated Moving Average (ARIMA) models, regression models, artificial neural networks (ANNs) are rarely applied in the field of fluvial river systems [11]. The uncertainty and complexity of the fluid systems associated with these models, particularly in the meandering river, are the main issues to be noted. The scales and directions of these changes in river migration are undefined and unidentified, requiring more quantitative data to predict channel morphology evolution in the reach of a river basin [12].

The ultimate goal of this research study was to understand and explain how the river morphology changes (bankline shifts) for Rapti river system for short-time prediction of river migration based on multi-temporal Landsat satellite imageries (2006-2019) and ARIMA model. This work was an attempt to predict the short-term morphological change (bankline shift) for 2020 in a very large scale (1:1000), that had not been often measured in earlier river morphological change modeling. This study is very useful for river management planning. The main objectives of this study were: (a) understanding the spatial and temporal change in river morphology of Rapti River System using 14 years Landsat satellite imageries; (b) identification of highly vulnerable sites based on frequency and magnitude of river bankline shifting, channel migration over the years, erosion / deposition pattern over the years; (c) prediction of river bankline on highly vulnerable sites using multi-temporal Landsat satellite imageries / ARIMA model; and (d) analysis of the relationship between water discharge, river bankline shifting rate, soil type, and sinuosity ratio.

The extensive bank erosion and river bank shifting in the Rapti River System has led to numerous social and economic consequences - loss of agricultural land (loss of livelihood), loss of housing and other essential infrastructure, displacement and involuntary migration giving rise to native migrant contest over limited resources in the basin. The government is putting a lot of effort to mitigate flood and erosion by constructing various river training structures. The results of the study would help in predicting the dynamics of the river in the future and taking up an adaptive policy considering climate change impacts to reduce the suffering of the riparian community due to morphological changes causing river erosion and flooding.

## 2. Literature Review

We have reviewed more than 50 important literatures on river morphology, prediction of bankline from 1977 to 2019, and summary of these literatures are presented in ascending chronological order (Table 1).

**Table 1.** Summary of Literature Review.

| S. No. | Year | Summary of Literature Review |
|---|---|---|
| 1 | 1977 | Keady et al. have developed a mathematical equation for prediction of migration rate of river. The influencing parameters are the slope of the river (s) and the amplitude of meander (A). Other variables involved in the equation are the gravity (g) and a function of the slope (Φ(s)) [13]. |
| 2 | 1980 | Hooke has analyzed the meander migration rate on rivers in Devon, England from field measurements. These measured rates were compared with the rates obtained from historical maps for the period from 1840 to 1975. He also compared the measured rates with published rates of bank erosion in the literature and found that the rate in his study followed the general trend of the worldwide values [14]. |
| 3 | 1982 | Brice has consisted of 43 data points from four different stream types (equiwidth, wide bend, braided point bar, braided) [15]. He has proposed that the erosion rate of the bank is related to the width of the channel, the equation: Y = 0.01 * B; where, Y (m/year): erosion rate, B (m): channel width. |
| 4 | 1983 | Nanson et al. have showed that the ratio of radius of curvature of a bend (Rc) to channel width (W) influences the lateral migration rate of a meandering river [16]. They have fixed the relationship between channel migration rate (MR) and the ratio of radius of curvature to channel width for the Beatton river, Canada. The normalized migration rate (MR/W) is highest when the ratio of radius of curvature to channel width (Rc/W) is about 3. |
| 5 | 1985 | Blondeaux et al. have developed and applied a two-dimensional (2D) model of flow and bed topography in sinuous channels with erodible boundaries in order to study the mechanism of meander initiation [17]. A resonance phenomenon uncovered by Ikeda et al. were detected when the values of relevant parameters fall within a certain range [18]. It was proposed that resonance controls the bend growth and is connected with bar instability. |
| 6 | 1990 | Pizzuto has developed a 2D numerical model to predict the distribution of boundary shear stress, cross-channel sediment transport rates, and evolution of bed topography [19]. The equilibrium values of a dimensionless depth increase as the bed slope decreases. |
| 7 | 1998 | Mosselman has developed a prediction method consists of a 2D depth-averaged flow model and a bank erosion model [20]. The prediction method is applied to a reach of the meandering gravel-bed river Ohre in the former state of Czechoslovakia. Poor agreement was observed. The author claims that inclusion of a 3D flow model, a sediment transport model, will improve the prediction results. |
| 8 | 1999 | Morphological changes in planform characteristics of Gorai river have been addressed by Sarker [21]. They were analyzed the erosion, accretion changes of sinuosity, planform changes, and meander migration of river. |
| 9 | 2000 | Clark et al., have studied the effect of land use change on channel morphology in north-eastern Puerto Rico [22]. They have started that the identification of reverse channel morphology along individual watercourses may be obscured in multi-watershed compilations in which other factors produce a consistent but scattered downstream trend. |
| 10 | 2001 | Duan et al., have developed a numerical-empirical model called Enhanced CCHE2D (EnCCHE2D) to simulate alluvial channel migration |

| S. No. | Year | Summary of Literature Review |
|---|---|---|
| | | phenomena [23-25]. The EnCCHE2D model is capable of predicting quasi-3D flow field and shear stress 30 distribution on the bed. |
| 11 | 2002 | A numerical method of river morphology for meander bends with erodible cohesive banks was developed by Darby [26]. Major features of the model are coupling of a 2D depth-averaged model of flow and bed topography with a mechanistic model of bank erosion, deposition of failed bank material debris at and its subsequent removal from the toe of the bank, and implementation of governing equations in moving boundary fitted coordinate system. |
| 12 | 2003 | Lagasse et al., have developed a methodology and ArcView tools for predicting channel migration includes ArcView 3.2-based bend measurement and channel migration predictor extensions, which provides a practical methodology to predict the rate and extent of meander migration through the use of sequential historic aerial photographs and maps [27]. |
| 13 | 2004 | Abad et al., have introduced a simplified river model for predicting river morpho-dynamics processes, including river migration [28]. The methodology consists of components such as designing stream restoration, linear and nonlinear analyses, and a plan form migration 33 model. |
| 14 | 2005 | Merwade et al., have developed an ArcGIS toolset (River Channel Morphology Model) for analysing and extrapolating river channel bathymetry [29]. The 3D representation of river channels described by RCMM can be used to run HEC-RAS model. |
| 15 | 2006 | Wang et al., have developed a methodology which has predicted the possible migration of a meander river including numerical simulation, modeling of migration, risk analysis, and development of a computer program [30]. |
| 16 | 2007 | Larsen et al., have studied the Sacramento river, California by using topographical map of 1904 and aerial photographs from 1937 to 1997 [31]. He has tracked temporal changes in river and bend geometry over the 93-year time interval. They have suggested that river length lost due to cut-off has been approximately made up for by progressive migration over the study period, but that the formation of high sinuosity bends susceptible to future cut-off may be on the decline. |
| 17 | 2008 | Kummu et al., have analysed the bank movement rate of Mekong river by using aerial photographs, SPOT-5 satellite imageries, and field survey data [32]. They have found that the average rate of bank erosion is slow in this river as compared to global scale; However, erosion rates were much higher for the islands in the river. |
| 18 | 2009 | Rana et al., have been calculated the sinuosity index and meander parameters like amplitude, wave-lengths of Rapti river in order to understand its departure from a straight course in the alluvial plain [33]. The method devised by Langbein et al., was used for analysis of spatial-temporal variation in the meander patterns [34]. |
| 19 | 2010 | An indirect method was established by Carvalho for the river morphology analysis by considering the spatial distribution of the sedimentary plumes [35]. Landsat-7 satellite imageries were used for river morphology analysis using an algorithm based on bands ratio index and bathymetric data. |
| 20 | 2011 | A hydrodynamic numerical model has been developed by Krapesch, which was supported by LiDAR data of the rivers [36]. This model can be analyzed the morphological effects of extreme floods and examines which parameters best describe the width changes due to erosion. |
| 21 | 2012 | The quantification of the actual bank erosion and deposition along the Brahmaputra river within India by an integrated approach was carried out by Sarkar using IRS satellite imageries [37]. The study highlighted several substantial facts about the changes in river morphology, stable and unstable reaches of the riverbanks and changes in the main channel course. |
| 22 | 2013 | Thian et al., have investigated the short-term and long-term channel migration along with the changing pattern of accretion, erosion and island dynamics for the braided and alluvial Jamuna River in the lower Brahmaputra using Landsat satellite imageries [38]. |
| 23 | 2014 | Yang et al., were employed the Landsat satellite imageries to quantify the planform migration of the reach from 1983 to 2013 and to investigate the possible effect of human activities on the lower Jingjiang reach channel evolution [39]. They have also introduced the migration direction to predict the future migration trends. |
| 24 | 2015 | Pourbakhshian et al., were presented a new stochastic method for predicting river morphological changes in near future [11]. Multi-variate regression equation based on channel bed height as a dependent parameter and three independent parameters daily flow, sediment discharge and bed slope, derivation of sediment rating curve equation using sediment concentration, and stream flow prediction using ARIMA stochastic modelling. |
| 25 | | Reza et al., were define the relations between riverbank line, bar growth and understanding the river morpho-dynamics of Padma river in Bangladesh using historical satellite imageries [40]. |
| 26 | | Fluvial-geomorphological changes of Bhagirathi-Hugli rivers in deltaic region of West Bengal were analyzed by Mallick using survey of India toposheets and several satellite imageries [41]. The pattern of different fluvial geomorphic features on the flood- plain, including meander cut-offs, oxbow lakes that hold rain water for an extended period, seasonal water bodies, active channels with considerable variability in turbidity and depth, decayed channels were identified. |
| 27 | 2016 | Landsat satellite images and mathematical technique through 2D numerical simulation were used by Bhuayan to predict morphological changes of Jamuna river in Bangladesh [42]. |
| 28 | | Nabi et al., have studied the bankline shifting of Meghna estuary, an active deltaic of Bangladesh using Rennell's map and Landsat satellite imageries from 1760 to 2014 [43]. This study produces high quality map of change detection of bankline shifting map of the study area across space and time. |
| 29 | | The hydraulic bank erosion rate with the help of analytical formulae and 2-dimensional morphological model was quantified by Khan using MIKE-21C platform powered by DHI [44]. The erosion rates thus obtained were compared to that revealed by satellite imagery. The erosion rates calculated by the used modelling approach was very close to the observed. |
| 30 | | A multi-dimensional hydrodynamic and sediment transport model (CCHE2D model) has been developed by Jia, which can analyse the widely varying channel plan form, morphology, and bed composition [45]. The hydrodynamic and sediment transport model is capable of adequately representing flow and sedimentation characteristics in river reaches containing hydraulic structures and complex channel geometry. |
| 31 | 2017 | Bank erosional and depositional pattern analysis was done by Rahman for delineation of course migration of the Padma river in Bangladesh using satellite images and GIS technologies [46]. A time-series of dry season satellite images during 1973-2009 were used to visualize the historical changes in morphology and to provide the basis for the long-term bank erosion process of the Padma river. |
| 32 | | Lai was developed the 2D morph-dynamic and bank erosion models coupled spatially and temporally through a special procedure, and a common mesh approach for vertical bed changes and lateral bank erosion [47]. |
| 33 | 2018 | Lant et al., have studied potential effect of the actively meandering Wabash river in Illinois, using a river migration model (RVR Meander) [48]. RVR Meander is a toolbox that can be used to model river channel meander migration with physically based bank erosion methods. This study assesses the Wabash river meandering processes through predictive modeling of natural meandering over the next 100 years, climate change effects through increased river flows, and bank protection measures. |

| S. No. | Year | Summary of Literature Review |
|---|---|---|
| 34 | 2019 | A procedure for the characterization of the temporal evolution of river morphology is presented by Spada [49]. They have used multi-temporal satellite imageries i.e. Corona, Landsat and Sentinel-2 from 1968 to 2017 to study the channel widths, active channel surface, water, vegetation and sinuosity indices. |
| 35 | | Akhter et al., have investigated spatiotemporal changes of channel morphology of the reach of Teesta river in Bangladesh during 1972-2031 using multi-temporal Landsat images data with GIS, spatial auto-correlation index, and an auto-regressive integrated moving average (ARIMA) model [50]. They have demonstrated that the temporal changes in channel shifting rates were mostly affected by high sedimentation in the river flow path. |
| 36 | | Pal et al., have addresses the planform dynamics of the Ganga river in the middle-lower portion over the last six decades and the evolution and transformation of the channel and its floodplain with the help of remote sensing and GIS techniques [51]. |
| 37 | | Sylvester et al., have studied the dynamics of meandering rivers and migration rates of more than 1600 bends of meandering rivers of Amazon basin using Landsat satellite images [52]. According to them bends with the highest curvatures show the highest migration rates; exceptions with limited migration seem to be related to the low erodibility of the outer bank. |
| 38 | | Pareta et al., have investigated multi-temporal changes in morphological and bank line migration for four rivers i.e. Bhagirathi, Mandakini, Alaknanda, and Kali rivers in Uttarakhand [10]. Bank line changes and river bar delineation have been obtained using high-resolution satellite data through GIS for the years 2005, 2010 and 2015. To assess the risk along critical vulnerable reaches, indicator-based approach is used. It will also be useful to drainage designers to plan the layout of drains and potential hydro projects and in planning of other infrastructure facilities like roads, national parks, reserve forest and government plans. |

## 3. Study Area Description

Rapti River is the largest tributary of Ghaghra River which is a major constituent of the Ganga. It extends from 26°18'00" N to 28°33'06" N and 81°33'00 E to 83°45'06" E and covers an area of 25,793 km$^2$ out of which 41% (10,642 km$^2$) lies in Nepal and 59% (15,151 km$^2$) in India. It rises at an elevation of 3048 m in Dregaunra Range of Nepal Siwalik and covers a total distance of 782 km (of which 565 km lies in lndia) before joining Ghaghra at Barhaj in Deoria district of Eastern Uttar Pradesh. The Rapti River flows through the districts of Bahraich, Shravasti, Balrampur, Siddharth Nagar, Sant Kabir Nagar, Gorakhpur and Deoria of Eastern Uttar Pradesh (Figure 1). The basin consists geologically of two distinct portions - structurally it is a segment of the great Indo-Gangetic trough and it has also some portion of the Himalaya's foothills region of the Siwalik. Recent findings of the chrono-association of the Gandak mega-fans areas revealed that the alluvia of the Old Rapti Plain (Burhi Rapti) is that of 5000 years before present, and that of Rapti is more than 500 years before present [53]. The objective is to predict short-term bankline shift in Rapti River (India site) using an empirical model (ARIMA model).

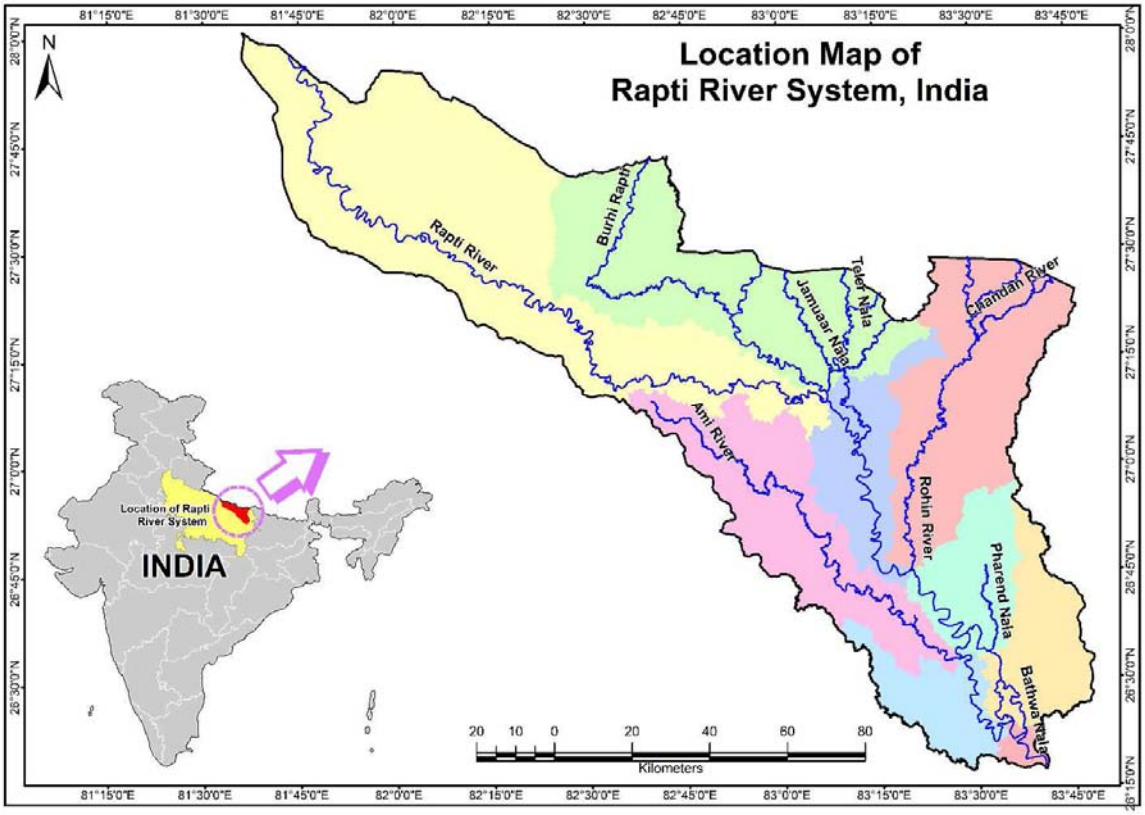


**Figure 1.** Location Map of Rapti River System, India.

# 4. Methodology and Data Used

## 4.1. Data Used and Sources

Pre-monsoon and moderate resolution Landsat satellite imageries i.e. Landsat-5 TM images (30m), Landsat-7 ETM$^+$ images (30m) and Landsat-8 OLI images (30m) from 2006 to 2019 were downloaded from Earth Explore, USGS (https://earthexplorer.usgs.gov). These multi-temporal satellite imageries were used to obtain information on river shifting and morphological trends of Rapti River and its 16 tributaries. The details of satellite remote sensing data with satellite names, sensors, paths/rows and acquisition dates are stated in Table 2. Other data used for this study are shown in Table 3.

**Table 2.** Time Series Satellite Remote Sensing Data Collection.

| S. No. | Year | Satellite | Sensor | Path/row | Acquisition Date |
|---|---|---|---|---|---|
| 1 | 2006 | Landsat-5 | TM | 142-041, 142-042, 143-041, 143-042 | 01st May 2006 |
| 2 | 2007 | Landsat-5 | TM | 142-041, 142-042, 143-041, 143-042 | 13th April 2007 |
| 3 | 2008 | Landsat-5 | TM | 142-041, 142-042, 143-041, 143-042 | 03rd May 2008 |
| 4 | 2009 | Landsat-5 | TM | 142-041, 142-042, 143-041, 143-042 | 06th May 2009 |
| 5 | 2010 | Landsat-5 | TM | 142-041, 142-042, 143-041, 143-042 | 16th April 2010 |
| 6 | 2011 | Landsat-5 | TM | 142-041, 142-042, 143-041, 143-042 | 12th May 2011 |
| 7 | 2012 | Landsat-7 | ETM$^+$ | 142-041, 142-042, 143-041, 143-042 | 06th May 2012 |
| 8 | 2013 | Landsat-8 | OLI | 142-041, 142-042, 143-041, 143-042 | 08th April 2013 |
| 9 | 2014 | Landsat-8 | OLI | 142-041, 142-042, 143-041, 143-042 | 15th March 2014 |
| 10 | 2015 | Landsat-8 | OLI | 142-041, 142-042, 143-041, 143-042 | 23rd May 2015 |
| 11 | 2016 | Landsat-8 | OLI | 142-041, 142-042, 143-041, 143-042 | 22nd April 2016 |
| 12 | 2017 | Landsat-8 | OLI | 142-041, 142-042, 143-041, 143-042 | 19th March 2017 |
| 13 | 2018 | Landsat-8 | OLI | 142-041, 142-042, 143-041, 143-042 | 15th March 2018 |
| 14 | 2019 | Landsat-8 | OLI | 142-041, 142-042, 143-041, 143-042 | 16th April 2019 |

**Table 3.** Other Data Sources.

| S. No. | Data Type | Data Sources and methodology |
|---|---|---|
| 1 | SoI Toposheet at 1:50,000 scale | Survey of India Toposheets, 2005<br>Toposheet No.: 63E/10, 14; 63I/02, 03, 07, 08, 11, 12, 16; 63J/09, 13, 14; 63M/08, 12; 63N/01, 02, 03, 05, 06, 07, 09, 10, 11, 14 & 15<br>Source: http://www.soinakshe.uk.gov.in |
| 2 | Elevation Data | ALOS PALSAR (DEM) Data: Advanced Land Observing Satellite (ALOS) Phased Array type L-band Synthetic Aperture Radar (PALSAR) Digital Elevation Model (DEM) Data with 12.5m spatial resolution.<br>Source: Alaska Satellite Facility, Fairbanks. U.S. state of Alaska. 2004-2015. Source: https://vertex.daac.asf.alaska.edu/ |
| 3 | Soil Data | Soil map has been collected from National Bureau of Soil Survey and Land Use Planning (NBSS&LUP), National Soil Survey, State Agricultural Department and updated through Landsat-8 OLI satellite remote sensing data with limited field check.<br>Source: https://www.nbsslup.in/publications.html |
| 4 | Water Discharge and Water Level Data | Daily water discharge data and water level data (from 2006 to 2019) has been collected from CWC (Central Water Commission) for 5 available gauging sites i.e. Birdghat, Balrampur, Kakrahi, Regauli, and Bhinga of the Rapti River System.<br>Source: http://cwc.gov.in/ |

## 4.2. ARIMA Model

Box et al., have developed an ARIMA model, which can produce accurate forecasts based on descriptions of historical pattern in the data, and best fit to a given time series and also satisfy the parsimony principle [54]. Their concept has fundamental importance on the area of time series analysis and forecasting [55]. Their methodology of Box does not assume any particular pattern in the historical data of the series to be forecasted. Rather, it uses a three-step iterative approach of model identification, parameter estimation and diagnostic checking to determine the best parsimonious model from a general class of ARIMA models [56]. This three-step process is repeated several times until a satisfactory model is finally selected (Figure 2). This model can be used for forecasting future values of the time series.

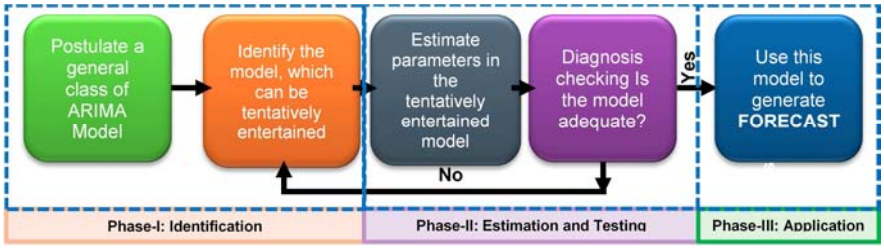


**Figure 2.** Schematic Representation of the Box-Jenkins Approach [57].

The ARIMA (Auto-Regressive Integrated Moving Average) model is the combination of auto-regression model and a

moving average model. The mathematical formulation of the ARIMA(p,d,q) model can be written as:

$$y_t = c + \phi_1 y_{t-1} + \cdots + \phi_p y_{t-p} + \theta_1 \varepsilon_{t-1} + \cdots + \theta_q \varepsilon_{t-q} + \varepsilon_t, \quad (1)$$

Where: $y_t$ is the differenced series (it may have been differenced more than once). The "predictors" on the right-hand side include both lagged values of $y_t$ and lagged errors. We call this an ARIMA(p,d,q) model.

p = order of the autoregressive part (AR) (p = periods to lag for eg: (if p= 3 then we will use the three previous periods of our time series in the autoregressive portion of the calculation) p helps adjust the line that is being fitted to forecast the series); d = degree of first differencing involved (d = in an ARIMA model we transform a time series into stationary one (series without trend or seasonality) using differencing. d refers to the number of differencing transformations required by the time series to get stationary); q = order of the moving average part (MA) (q = this variable denotes the lag of the error component, where error component is a part of the time series not explained by trend or seasonality).

In this study, we have used the ARIMA $(p,0,q)x(P,1,Q)_{12}$ with constant model. If we add the indicated MA(1) and SMA(1) terms to the preceding model, we obtain an ARIMA(1,0,1)x(0,1,1) model with constant, whose forecasting equation is:

$$Y_t = \mu + Y_{t-12} + \phi_1(Y_{t-1} - Y_{t-13}) - \theta_1 e_{t-1} - \Theta_1 e_{t-12} + \theta_1 \Theta_1 e_{t-13} \quad (2)$$

The ARIMA $(1,0,1) \times (0,1,1)_{12}$ model is chosen using error evaluation standards such as MAE, MSE, and RMSE. It is evident that the estimated values are close to the observed values in the Rapti river system which proved to be model suitability. In fact, the geomorphological phenomena of time series analysis are quite difficult to obtain accurate values. The justification for using the ARIMA model is that it is one of the most popular and extensively applied stochastic time series models, proving successful in the study of geomorphology [11]. This model has gained a lot of attention due to its simplicity in understanding and implementation due to its flexibility to represent multiple varieties of time series with simplicity [55].

# 5. Result

## 5.1. Priority Vulnerable Sites

One hundred and five priority vulnerable sites were identified for analysis, morphology modelling for predicting changes, and conducting field assessments. The multi-temporal remote sensing data from 2006 to 2019 have been digitized in shapefiles using Esri ArcGIS-10.5 software. The river course and silt deposit areas in India side were delineated.

To identify the priority vulnerable locations from the temporal analysis of the satellite imageries, certain criteria were used. They are - (i) frequency and magnitude of river bankline shifting, (ii) channel migration over the years, (iii) erosion / deposition pattern over the years and (iv) presence of critical flood management assets like barrages, bridges, launching aprons, rain cuts, regulator inlets outlets, spur structures, and embankment structures. By using these criteria, 105 vulnerable sites in the Rapti River System were identified. The locations of priority vulnerable sites are shown in Figure 3.

## 5.2. River Bank Erosion and Deposition Areas Analysis

Erosion plays a significant role in the changing environment of a river. It affects water flow, water quality, channel width and depth and safe use of a river as a transportation corridor. Generally, river bank erosion or deposition is a mechanism of sediment (bank material) transportation by a river that affects the river channel courses [58]. Fluvial geomorphic processes are very active in most of the rivers in north India. As a result, river erosion is common in the study area, Rapti River and its 16 tributaries.

Multi-temporal Landsat satellite remote sensing data from 2006 to 2019 have been used for this analysis. The two resultant shapefiles were superimposed in-order-to demarcate union wise erosion and deposition areas. The high erosion and higher bar deposition areas were also identified, which have been verified in field. The total area of erosion and deposition from all the unions were calculate by using ArcGIS software. The erosion and deposition area of Rapti river system has been extracted of years 2006 to 2018 and shown in Table 4.

The morphology and behavior of Rapti river undergo drastic changes in response to various flow regime. The erosion and flood are a common phenomenon in Rapti river, but it becomes a matter of serious concern when it takes the form of disaster. The study area is also prone to devastating floods. But due to severe erosion of bankline with floods, the situation in the area is critical. During the monsoon season, the rivers coming from the hills bring huge amount of water and sediment and fill the entire channel area. Due to this it affects the stability of channels and banklines.

**Table 4.** Erosion and Deposition Area (2006 - 2019) in Rapti River System.

| | Erosion and Deposition Area ($Km^2$) | | | | | | | | | | | | |
|---|---|---|---|---|---|---|---|---|---|---|---|---|---|
| | 2006-2007 | 2007-2008 | 2008-2009 | 2009-2010 | 2010-2011 | 2011-2012 | 2012-2013 | 2013-2014 | 2014-2015 | 2015-2016 | 2016-2017 | 2017-2018 | 2018-2019 |
| Deposition | 33.27 | 31.60 | 43.43 | 21.29 | 41.02 | 35.92 | 24.29 | 22.28 | 41.25 | 29.06 | 16.09 | 34.12 | 31.13 |
| Erosion | 24.91 | 42.95 | 30.95 | 45.26 | 21.71 | 31.08 | 25.57 | 41.98 | 22.61 | 24.19 | 52.29 | 46.79 | 34.19 |

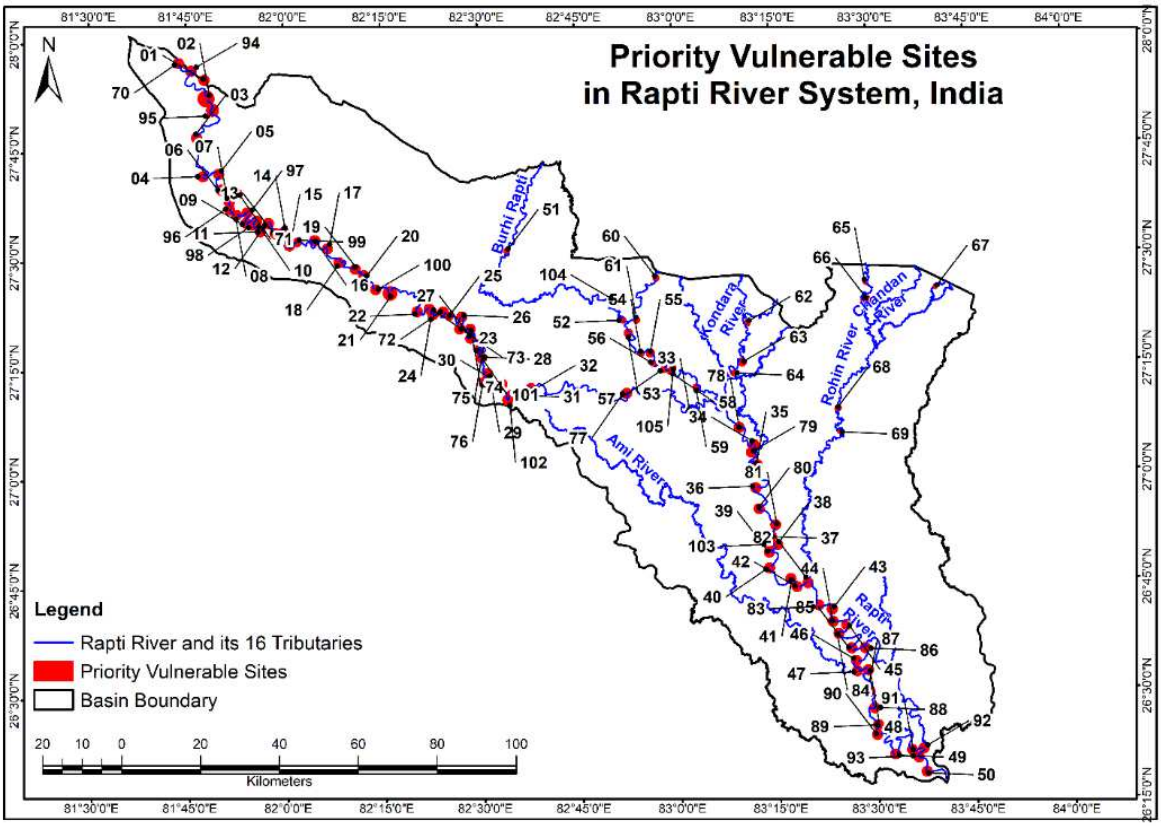


**Figure 3.** Priority Vulnerable Sites in Rapti River System in India.

## 5.3. River Bankline Shift Analysis

The Rapti river and its tributaries are constantly changing due to the geomorphic (e.g. water velocity), climate agents (e.g. flooding) and human activities (e.g. sand excavation, removal of vegetation cover and fertile soil excavation). The gradient (or slope), the amount of water, the velocity of water and the nature of a river or tributary are the parameters due to changes in the shape and size of a river / tributary [59]. The GIS technique (spatio-temporal analysis of satellite imagery) using advanced remote sensing data over the last 14 years has been used to identify changes in river course (both river and tributaries) and further calculations have had analysed river shifting and bank erosion. The bankline of Rapti river and 16 tributaries have been manually digitized from 2006 to 2019 by using multi-temporal Landsat satellite imageries i.e. Landsat-5 TM, Landsat-7 ETM+, and Landsat-8 OLI. By overlaying this database locations of bank channel shifting of Rapti river and tributaries have been identified. The shifted parts of the river have been mapped by vectorisations in GIS. A conceptual diagram of river bank line shift analysis is shown in Figure 4.

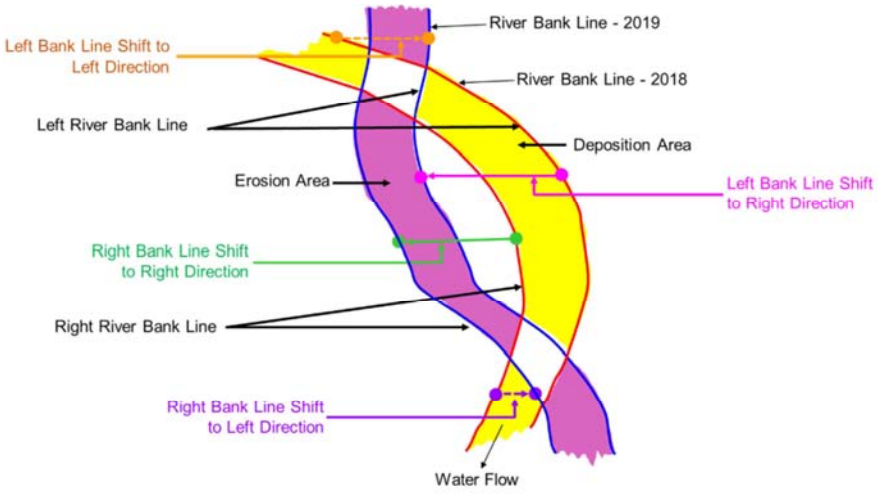


**Figure 4.** A Conceptual Diagram for River Bankline Shift Analysis.

We have fixed 31 cross-section lines at every vulnerable site, and river bank line shift has been measured for 105 vulnerable sites. The bank line shift has been measured in both bank lines i.e. right bank line and left bank line (where the vulnerable site is situated) with reference to length (in metres) and direction from 2006 to 2019. A positive value (+) indicates that the river bank line has shifted in the right direction from previous year, while a negative value (-) indicates that the river bank line has shifted in the left direction from previous year. After a detailed study of river bank line shift data of Rapti river system, we have observed a relationship between erosion / deposition and bankline shifting, which is shown in Table 5.

**Table 5.** Relationship between Erosion, Deposition and Bankline Shift.

| S. No. | From previous year to next year | Remarks |
|---|---|---|
| 1 | Right bankline shift to left direction | Deposition |
| 2 | Right bankline shift to right direction | Erosion |
| 3 | Left bankline shift to left direction | Erosion |
| 4 | Left bankline shift to right direction | Deposition |

A river cross section can be defined as the change of river depth (elevation) in relation to the horizontal distance from one river to another bank. Total 31 cross-sections for each vulnerable site have been demarcated perpendicular to the river (year 2019), and separation of cross-sections is 100 meters. We have measured river bank line shift at 3255 locations (105 vulnerable sites x 31 cross-sections = 3255 locations) in Rapti river system. In this study, we have analysed and used only two vulnerable sites data (Site No. 05, and Site No. 33) for prediction of bank line change.

## 5.4. Time Series Modeling and Forecasting

Bank erosion (accretion) and / or river movement modeling based on exceeding a critical threshold becomes unstable for short-term simulations, giving rise to local problems of widening or narrowing at unrealistic values. Furthermore, the results struggle to handle the system's response to cutoffs [60-61]. To solve these problems, a statistical approach has been applied. Time-series generated for various river morphometric attributes from multi-temporal satellite image analysis (pre-monsoon only) has been used. Other data from satellite imagery i.e. erosion / deposition, sinuosity ratio; discharge data, and soil data have been used for correlation of model output data.

The time-series of these morphometrics are divided into two sets, (i) Set-1: 80% of the time-series has been used for the calibration of model, (ii) Set-2: 20% of the time-series has been used for validation of the forecast model. An ARIMA $(1,0,1)x(0,1,1)_{12}$ model has been used to predict the short-term morphological change in Rapti river system. Validation assessment approach measures the fit between model predictions and satellite data of that predicted year. We have compared the river bank line data from satellite imagery and model output for 2018 and 2019 with the error of + 15 m (half size of a pixel in Landsat-8 OLI satellite imagery). Validation of ARIMA model output vs satellite data for site no. 05, and site no. 33 is shown in Figure 5, and Figure 6 respectively.

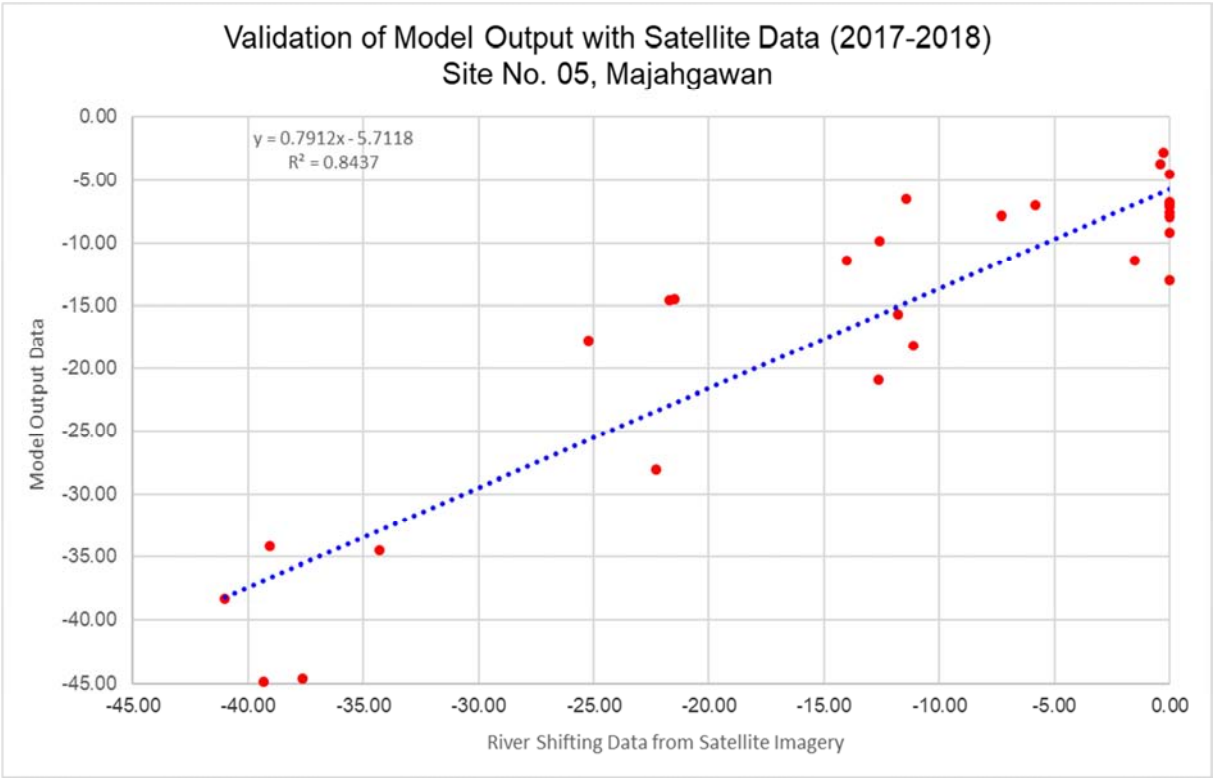

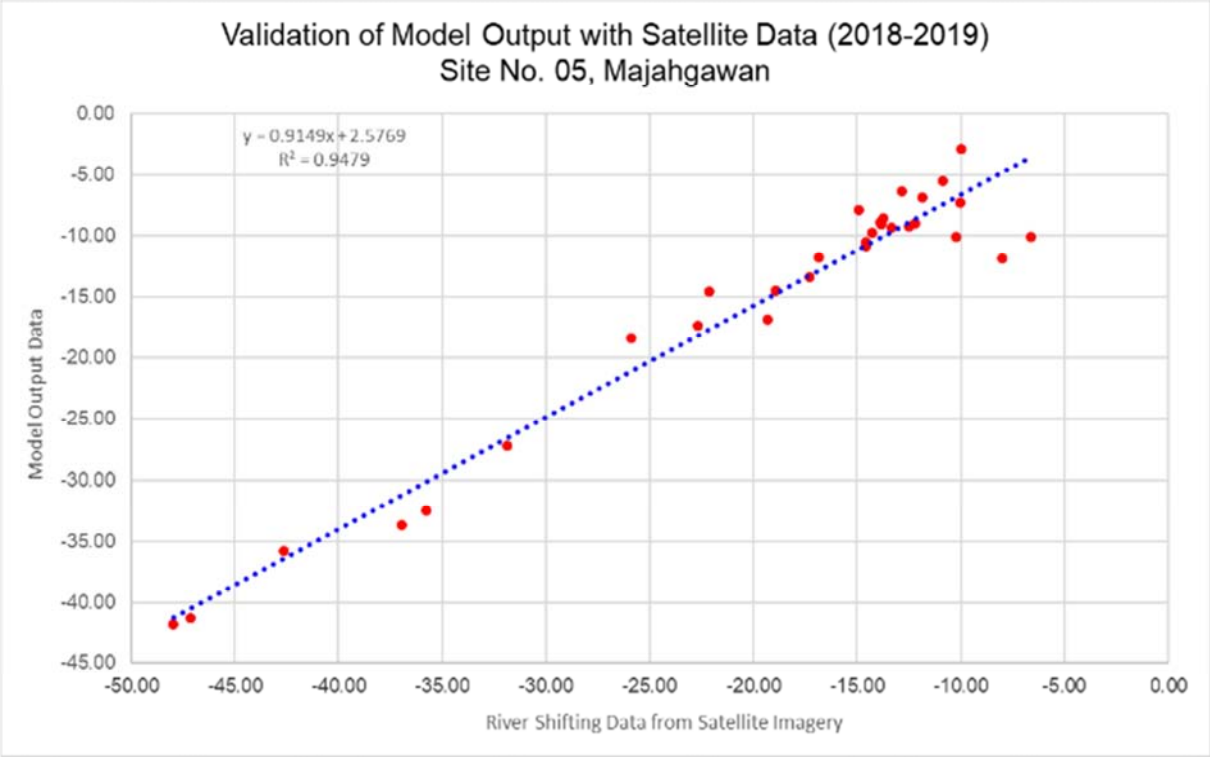


**Figure 5.** Validation of Model Output with Satellite Data for Site No. 05, Majahgawan.

The projection of Rapti river at site no. 05 is NE (Figure 8). The average shifting rate (2006 to 2019) in this direction is 12.03 m per year. The validation of model output versus satellite imagery has an accuracy of 90%.

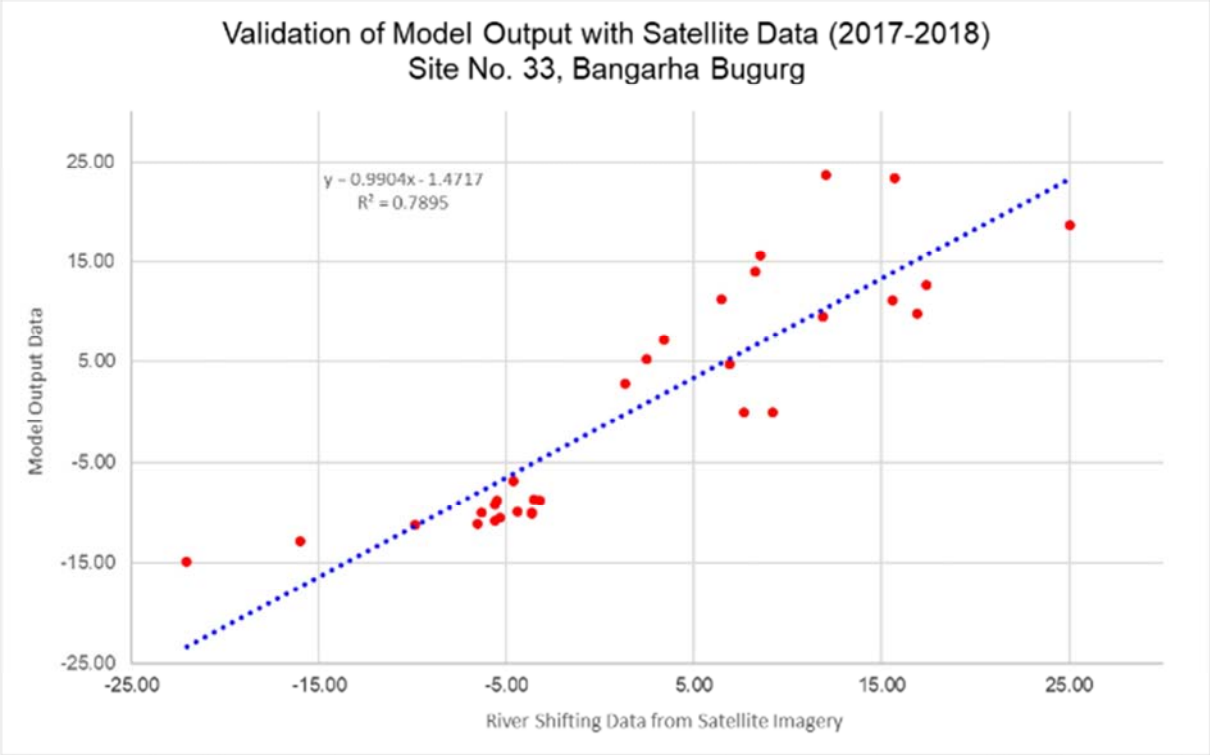

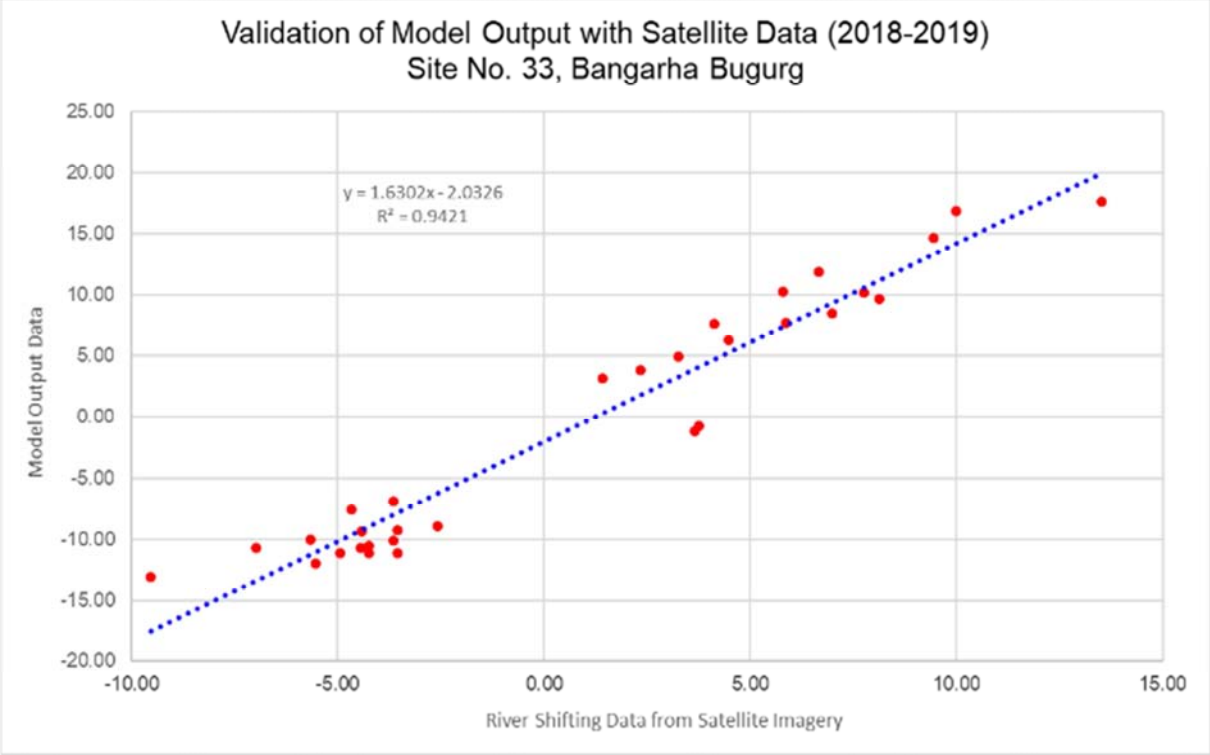


**Figure 6.** Validation of Model Output with Satellite Data for Site No. 33, Bangarha Bugurg.

The projection of Rapti River at site no. 33 is SW (Figure 9). The average shifting rate (2006 to 2019) is 5.17 m per year. The validation of model output versus satellite imagery has an accuracy of 87%.

### 5.4.1. Equation for Generation of Predicted Points (x, y)

By using the ARIMA (1,0,1) x $(0,1,1)_{12}$ model, we have extracted the predicted distance from 2019 (bankline from satellite imagery) to 2020 (ARIMA model output), but our concern is how to draw this distance in GIS. To solve the problem, an equation has been produced, which can draw the distance in GIS from 2019 to 2020, and generate the x, y coordinate of model output at each cross-section line. The mathematical explanation is shown in Figure 7.

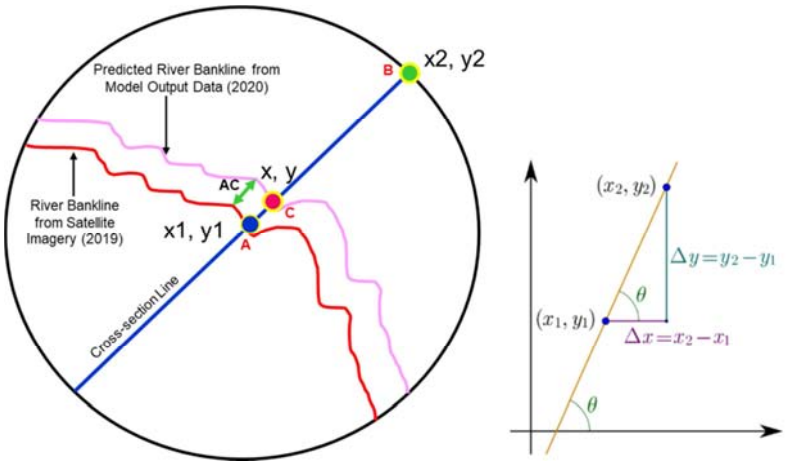


**Figure 7.** Conceptual Diagram for Generation of Predicted Points (x, y).

For measurement of slope between x1y1 and x2y2 or x1y1 and xy; the below stated equations have been used.

$$\text{Slope (m)} = y2 - y1 \,/\, x2 - x1 \quad (3)$$

In equation (3) we can generate the coordinate of x1y1 and x2y2 in GIS.

$$\text{Slope (m)} = y - y1 \,/\, x - x1 \quad (4)$$

Equation (4) can be written as Equation (5)

$$y - y1 = \text{Slope (m)} * (x - x1) \quad (5)$$

For measurement of distance between point (A) and point (B), the below stated equation has been used.

$$\text{Distance (AB)} = \sqrt{(x2 - x1)^2 + (y2 - y1)^2} \quad (6)$$

The same equation can be used for measurement of distance between point (A) and point (C)

$$\text{Distance (AC)} = \sqrt{(x - x1)^2 + (y - y1)^2} \quad (7)$$

Equation (7) can be written as Equation (8)

$$[\text{Distance (AC)}]^2 = (x - x1)^2 + [\text{Slope (m)} * (x - x1)]^2 \quad (8)$$

Equation (8) can be written as Equation (9)

$$[\text{Distance (AC)}]^2 = (x - x1)^2 + \text{Slope (m)}^2 * (x - x1)^2 \quad (9)$$

Equation (9) can be written as Equation (10)

$$[\text{Distance (AC)}]^2 = (x - x1)^2 * [1 + m^2] \quad (10)$$

Equation (10) can be written as Equation (11)

$$(x - x1)^2 = AC^2 / (1 + m^2) \quad (11)$$

Equation (11) can be written as Equation (12)

$$x - x1 = \sqrt{[AC^2 / (1 + m^2)]} \quad (12)$$

Equation (12) can be written as Equation (13)

$$x = \sqrt{[AC^2 / (1 + m^2)]} + x1 \quad (13)$$

Distance between A&C has been extracted from ARIMA model; m is slope, which has been calculated by using x1y1 and x2y2 coordinate. If, we put these two values in equation (13), the coordinate of x can be generated.

Equation (5) can be written as Equation (14)

$$y = [\text{Slope (m)} * (x - x1)] + y1 \quad (14)$$

In Equation (14), Slope (m) has been calculated by using x1y1 and x2y2 coordinate, Coordinate of (x) has been obtain from Equation (13), and Coordinate of x1y1 has been generated in GIS.

By using these equations, we have generated predicted points for all 105 vulnerable sites. By using this method, we have predicted the bankline shifting for years 2018, 2019, and 2020 for all 105 sites, but here we are showing site no. 5 and site no. 33 in Figure 8 and Figure 9, respectively.

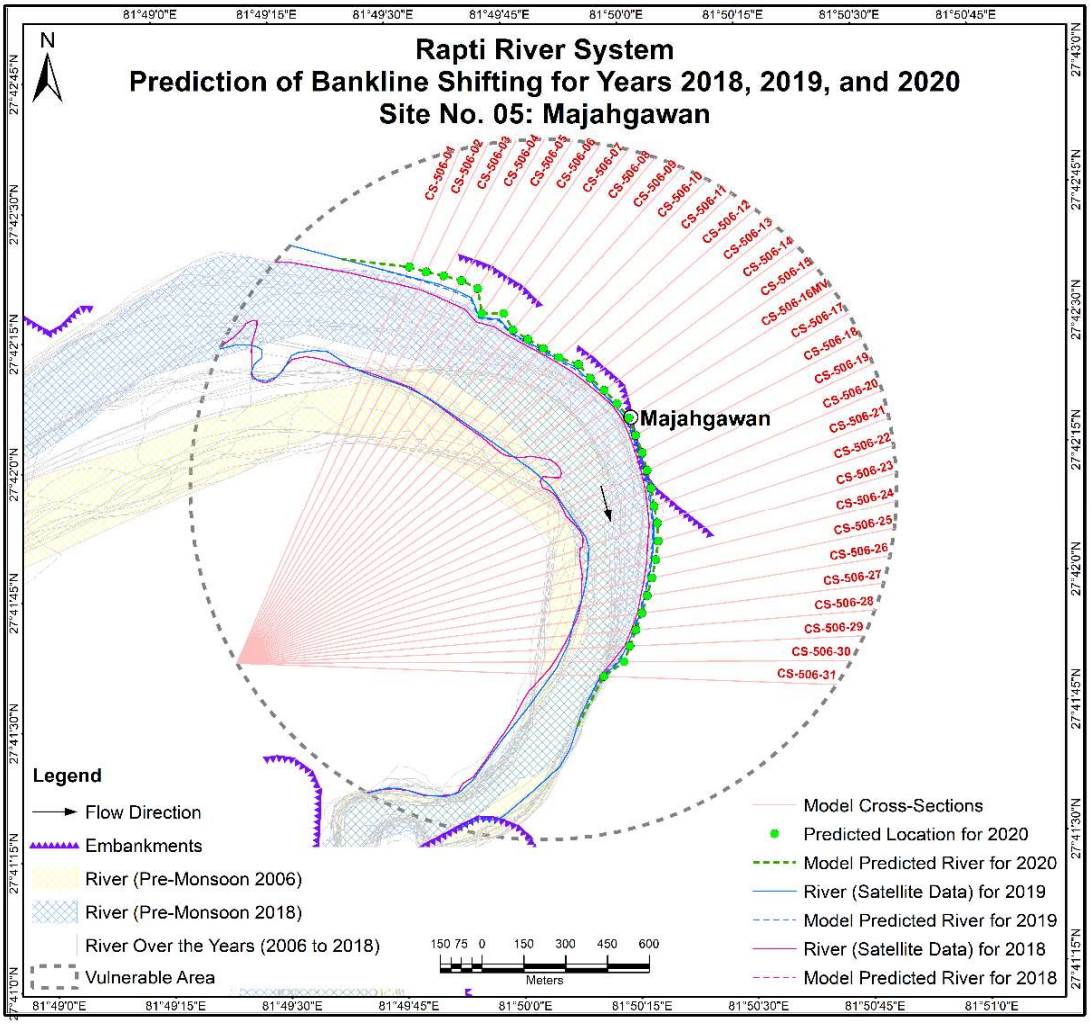


**Figure 8.** Prediction of Bankline Shifting for Years 2018, 2019, and 2020 of Site No. 05, Majahgawan.

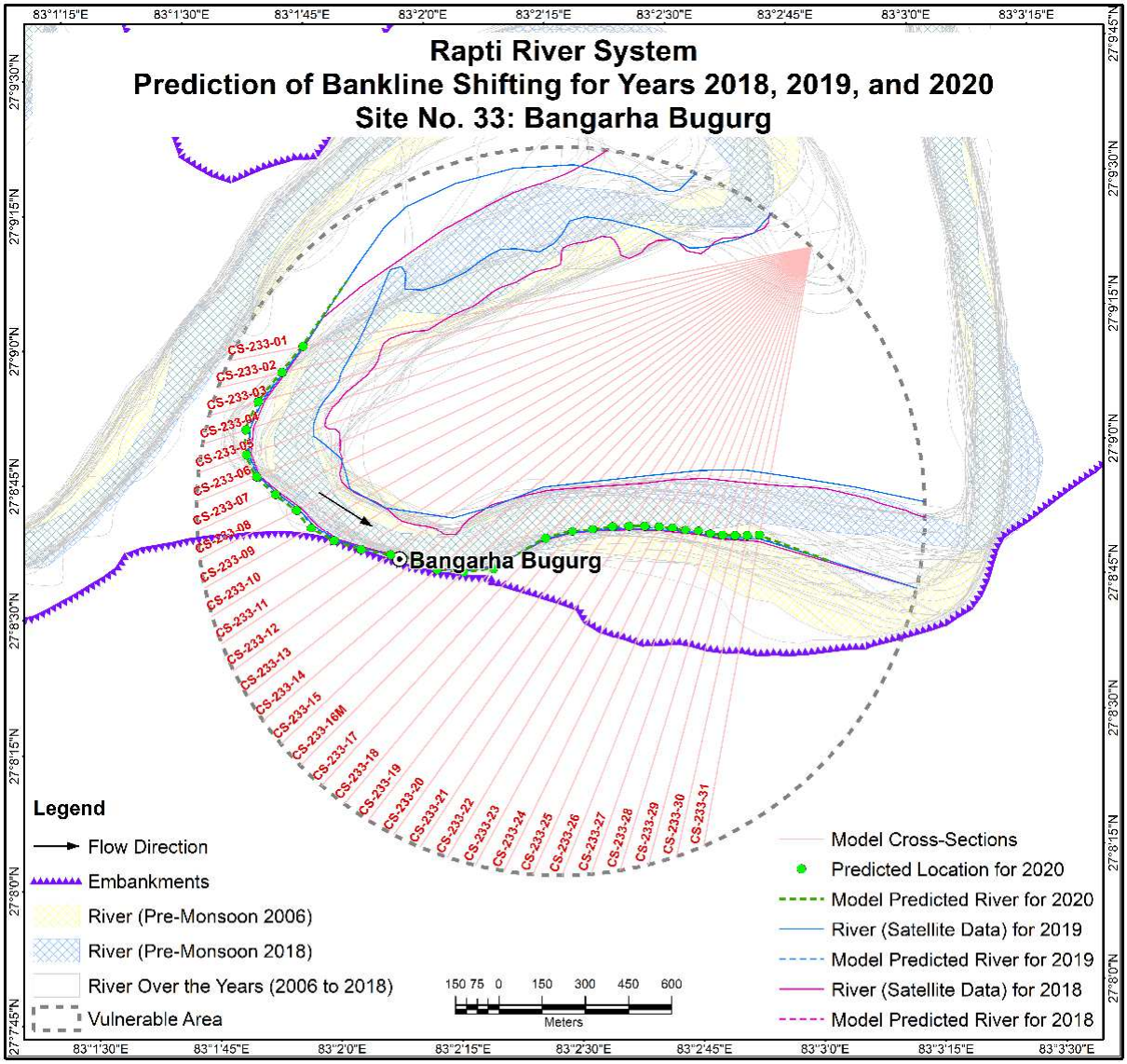


**Figure 9.** Prediction of Bankline Shifting for Years 2018, 2019, and 2020 of Site No. 33, Bangarha Bugurg.

### 5.4.2. Limitations of ARIMA Model

Empirical equations which relate hydrologic and geomorphic channel characteristics offer a way to estimate and predict meander river dimensions, reducing the extensive data needs of planimetric assessments. However, the empirical models which have been developed appear to exhibit site-specific nature apparent in planimetric assessments. The following points are considered as limitations of the empirically-based model:

The river bank line has an error of + 15 m due to the size of half a pixel in Landsat satellite imageries.

This model is based on past condition, if there are any future human intervention from present condition i.e. establishment of new embankment, stud structure, spur structure, porcupine structures, cutter and any other anti-erosion or river training work, then the model will not show the accurate result.

## 6. Discussion

### 6.1. Relationship Between Soil Type and River Bankline Shifting Rate

The field assessments in the Rapti river system found that the soils of the river banks comprise clay, clay loam, sandy loam, loamy sand and sand, of which sandy loam, loamy sand and sand are non-cohesive, loose and more common. The size of the soil particles (sand size or smaller) and the percentages of sand, silt and clay in the soil are influenced by bank erosion and the percentage of sand is greater in areas of significant river bank erosion. Steepness of the river bank, the nature of bank material and the presence or absence of deep roots of vegetation have great implication on bank erosion and thereby the lateral shifting of the river. Lateral shifting is a common feature of meandering channel and therefore, it becomes an

important determinant of the nature of shifting of the Rapti River and its tributaries. Among the selected vulnerable sites, the lateral shifting is highest at Site No. 02 Laxmanpur Kothi, and lowest at Site No. 49 Majhawaliya.

Statistical analysis of average river bankline shifting rate at each vulnerable site (2006 to 2019) has been carried out and compared to river bank soil type. Average river bankline shifting rate in m per year is listed against soil type / bank material from 2006 to 2019 in Table 6 and shown in Figure 10.

**Table 6.** Soil Type / Bank Material wise Average River Bankline Shifting Rate (2006 to 2019).

| S. No. | Soil Type / Bank Material | Average River Bankline shifting rate (m) / year (2006 to 2019) |
|---|---|---|
| 1 | Clay | 8.899 |
| 2 | Clay loam | 8.477 |
| 3 | Embanked | 10.462 |
| 4 | Loamy sand | 12.545 |
| 5 | Sand | 31.000 |
| 6 | Sandy loam | 27.613 |

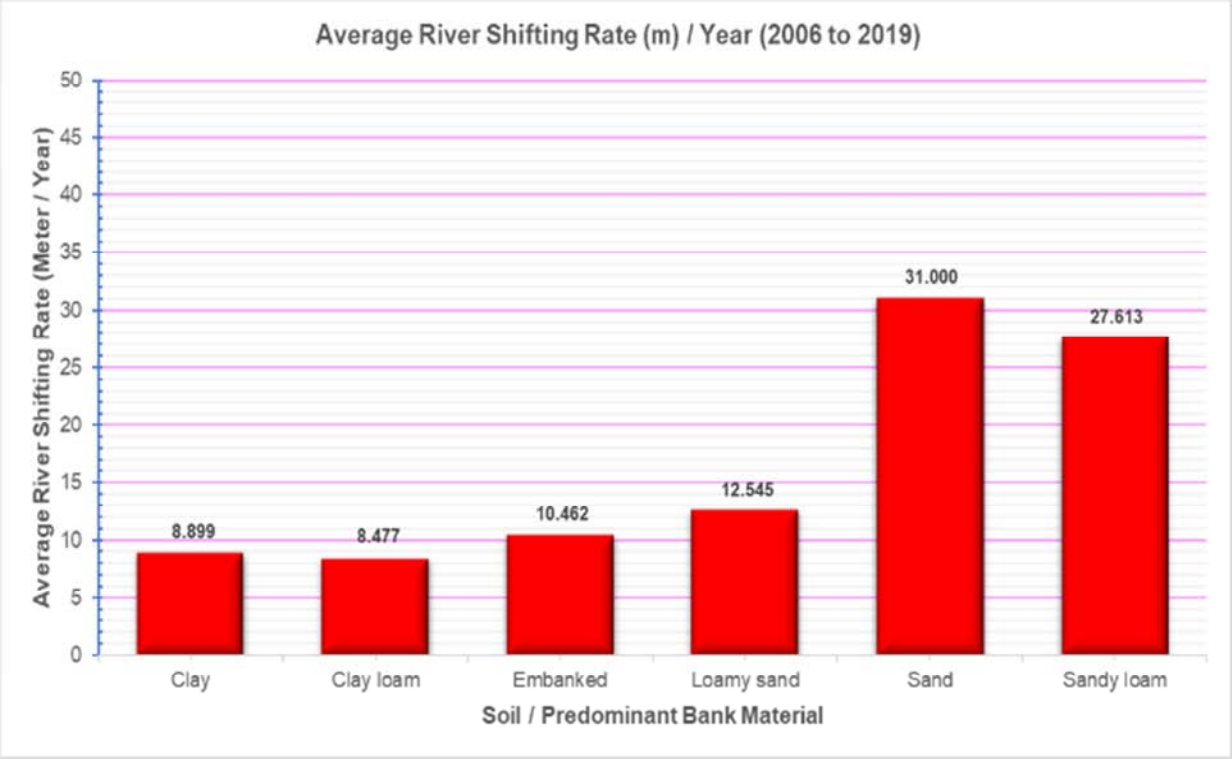


**Figure 10.** Soil Type / Bank Material wise Average River Bankline Shifting Rate (2006 to 2019).

The Rapti river has changed its course over the last 20 years, with vast erosion of the river bank, especially after the 1998 flood [62]. Figure 10 shows that the river bankline shifting rate is very high in sand and sandy loam, then loamy sand, while river bankline shifting rate is lower in clay and clay loam. Earth and not visible bank material are not plotted on the graph due to absence of soil type / bank material. The morphology and behaviour of Rapti river undergo drastic changes in response to various flow regimes. The bankline of the Rapti river is very un-stable and bank failure is rampant in many vulnerable areas along the river during the monsoon season. These failures seem to be a function of hydraulic character of flow and engineering properties of bank materials.

## 6.2. Relationship Between Soil Type, Sinuosity Ratio and River Bankline Shifting Rate

The sinuosity of a channel can be defined as the complexity or curvilinearity displayed within a meandering channel [63-64]. Sinuosity is commonly expressed as the ratio between the length along a channel ($L_C$) and the length of the valley ($L_V$) within a given reach [65]. The sinuosity ratio for the Rapti river system ranges from 1.478 to 2.387. The average sinuosity ratio of the Rapti river is 1.848 [66].

To compare sinuosity ratio with soil type / bank material and average river bankline shifting rate, we have calculated the sinuosity ratio for each vulnerable area by using the channel length ($L_C$) and valley length ($L_V$) for 2019. The comparison

of soil type, sinuosity ratio and river bankline shifting rate is shown in Table 7 and plotted in Figure 11.

**Table 7.** Soil Type / Bank Material vs. Average River Bankline Shifting Rate vs. Average Sinuosity Ratio.

| S. No. | Soil Type / Bank Material | Soil Type / Bank Material wise Average River Bankline Shifting Rate (m) / Year | Soil Type / Bank Material wise Average Sinuosity Ratio |
|---|---|---|---|
| 1 | Clay | 8.899 | 1.762 |
| 2 | Clay loam | 8.477 | 1.819 |
| 3 | Embanked | 10.462 | 2.241 |
| 4 | Loamy sand | 12.545 | 1.773 |
| 5 | Sand | 31.000 | 2.831 |
| 6 | Sandy loam | 27.613 | 1.264 |

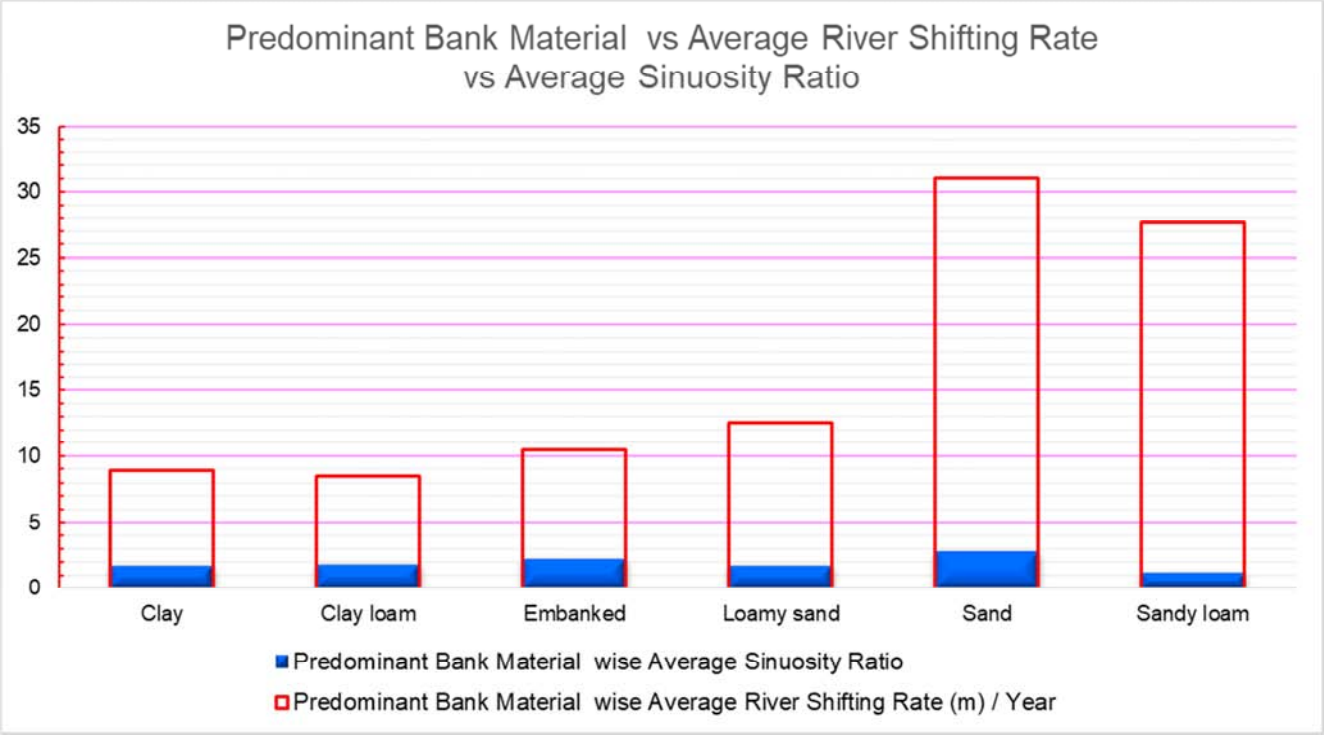


**Figure 11.** Soil Type / Bank Material vs. Average River Bankline Shifting Rate vs. Average Sinuosity Ratio.

Meandering rivers (sinuosity >1.5) have series of turns with alternate curvatures connected at the points of inflection or by short straight crossings [67]. They have a relatively low gradient. Naturally meandering rivers are quite unstable due to predominant bank erosion of concave banks [68]. The outer concave edge bends and there is deep flow with high velocity. The depth of flow at the crossing is relatively shallow compared to bends [69]. Figure 11 shows that the sinuosity ratio is high in sand, clay loam and loamy sand, which is directly related to river bankline shifting rate. In consequence sinuosity ratio is high, when river bankline shifting ratio is high as generally occurring in sandy soil.

### 6.3. Relationship Between Water Discharge, River Bankline Shifting Rate, Soil Type, and Sinuosity Ratio

The water discharge and water level data are available for 5 gauging sites i.e. Birdghat, Balrampur, Kakrahi, Regauli, and Bhinga of the Rapti river system only for monsoonal season from June to October (2006-2019). The location map of water discharge stations and water level data stations is shown in Figure 12. Ten-daily hydrographs and rating curves (water level vs discharge) have been prepared to depict the river flow characteristics.

Figure 13 shows the mean flows at various locations along Rapti river system between 2006 and 2019. The flow at Kakrahi, in the Burhi Rapti tributary, is the lowest. The highest flow is in the Rapti river at Birdghat, which is the most downstream station. This is closely followed by the next station upstream which is Regauli. Bhinga and Balrampur have very similar mean flows due to their proximity and being upstream the flow is much lower. Within the monsoon season, the maximum flow in the Rapti river system is observed in the last-third of August. A comparision table of water discharge, river bankline shifting rate, soil type and sinuosity ratio for the five stations are given in Table 8.

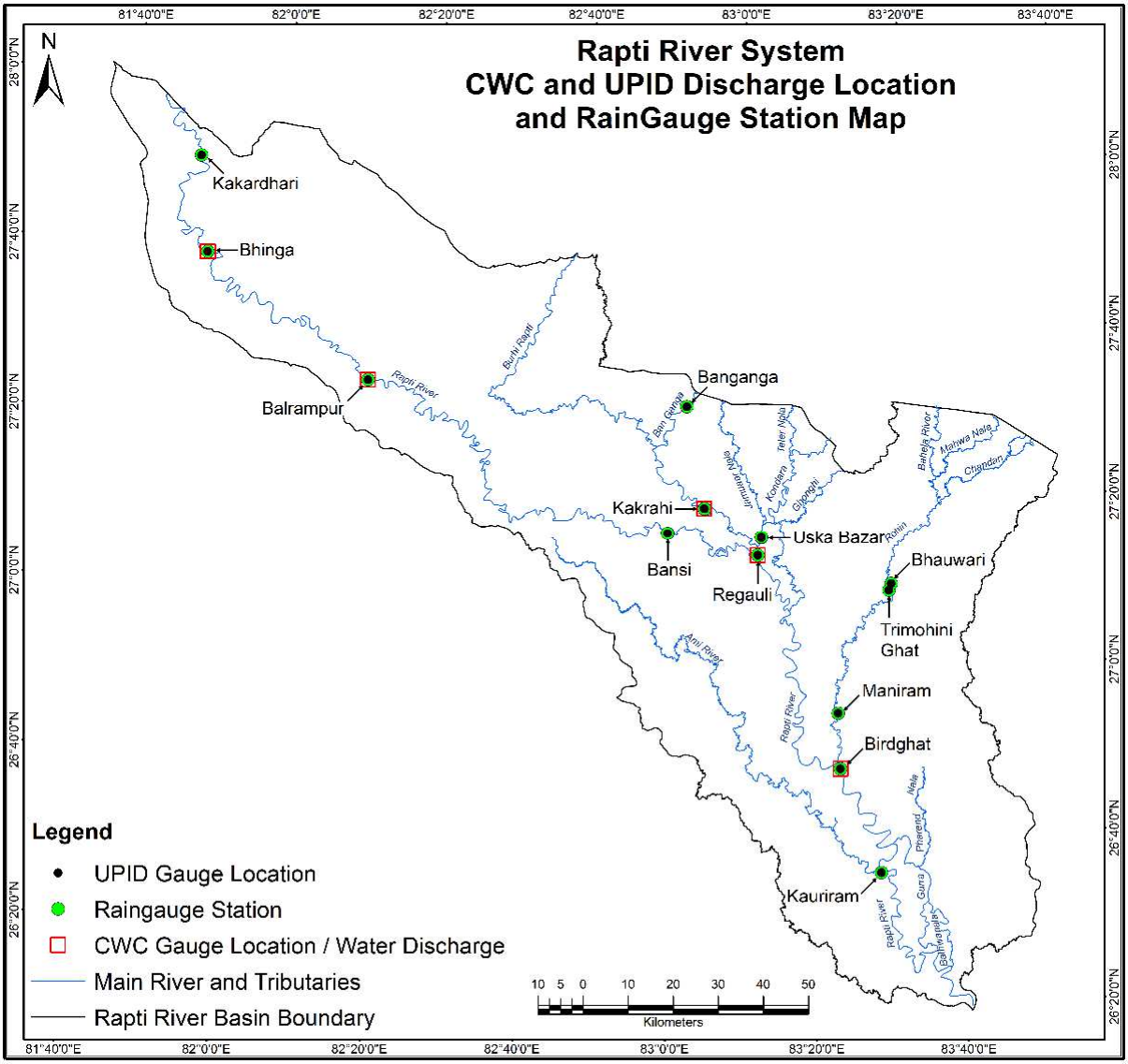


**Figure 12.** Location Map of Water Discharge Stations and Water Level Data Stations.

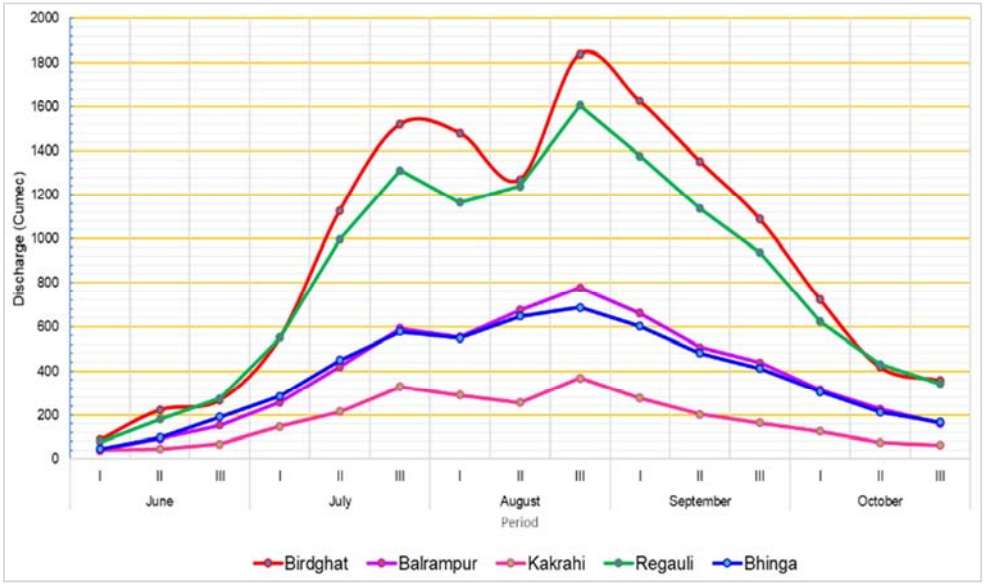


**Figure 13.** Mean Flows at Various Locations along Rapti river (2006-2019).

**Table 8.** Summarized the data of Water Discharge, River Bankline Shifting Rate, Soil Type, and Sinuosity Ratio.

| Water-Discharge Stations and Site No | Years | Max 10-daily Discharge (Cumec) | Average River Bankline Shifting Rate (m) | Soil Type / Bank Material | Sinuosity Ratio |
|---|---|---|---|---|---|
| Balrampur and Site No. 05 | 2006 | 586.70 | | Sandy loam | 1.46 |
| | 2007 | 1,197.54 | 10.96 | | |
| | 2008 | 1,282.94 | 5.18 | | |
| | 2009 | 1,002.64 | 5.13 | | |
| | 2010 | 971.16 | 10.66 | | |
| | 2011 | 754.76 | 2.21 | | |
| | 2012 | 971.31 | 18.31 | | |
| | 2013 | 1,027.82 | 43.40 | | |
| | 2014 | 1,184.10 | 0.00 | | |
| | 2015 | 648.05 | 6.12 | | |
| | 2016 | 1003.73 | 13.47 | | |
| | 2017 | 999.56 | 13.42 | | |
| | 2018 | 786.13 | 0.00 | | |
| | 2019 | 1025.15 | 13.27 | | |
| Bhinga and Site No. 18 | 2006 | 576.16 | | Loamy sand | 1.29 |
| | 2007 | 1,011.96 | 10.36 | | |
| | 2008 | 713.16 | 10.63 | | |
| | 2009 | 996.95 | 0.00 | | |
| | 2010 | 939.31 | 2.32 | | |
| | 2011 | 759.44 | 0.00 | | |
| | 2012 | 955.43 | 0.00 | | |
| | 2013 | 901.43 | 0.00 | | |
| | 2014 | 1,054.65 | 0.00 | | |
| | 2015 | 532.79 | 0.00 | | |
| | 2016 | 786.23 | 5.45 | | |
| | 2017 | 803.42 | 11.52 | | |
| | 2018 | 923.09 | 20.61 | | |
| | 2019 | 798.19 | 7.98 | | |
| Birdghat and Site No. 58 | 2006 | 1,302.45 | | Clay | 1.61 |
| | 2007 | 5,896.91 | 18.23 | | |
| | 2008 | 4,383.03 | 1.82 | | |
| | 2009 | 2,745.36 | 0.08 | | |
| | 2010 | 1,775.76 | 2.05 | | |
| | 2011 | 764.36 | 0.00 | | |
| | 2012 | 857.04 | 0.00 | | |
| | 2013 | 2,166.52 | 0.72 | | |
| | 2014 | 2,295.89 | 5.81 | | |
| | 2015 | 503.78 | 0.00 | | |
| | 2016 | 779.65 | 2.29 | | |
| | 2017 | 805.13 | 5.73 | | |
| | 2018 | 823.54 | 8.58 | | |
| | 2019 | 767.71 | 3.38 | | |
| Kakrahi, and Site No. 33, 59 | 2006 | 427.84 | | Loamy sand | 3.47 |
| | 2007 | 756.89 | 17.28 | | |
| | 2008 | 780.98 | 13.65 | | |
| | 2009 | 662.33 | 11.89 | | |
| | 2010 | 494.45 | 3.54 | | |
| | 2011 | 341.71 | 0.00 | | |
| | 2012 | 425.85 | 0.00 | | |
| | 2013 | 423.47 | 4.89 | | |
| | 2014 | 438.02 | 8.25 | | |
| | 2015 | 115.50 | 0.00 | | |
| | 2016 | 503.13 | 0.57 | | |
| | 2017 | 444.44 | 8.88 | | |
| | 2018 | 519.09 | 13.67 | | |
| | 2019 | 475.53 | 4.32 | | |
| Regauli, and Site No. 42 | 2006 | 1,352.13 | | Embanked (Loamy sand) | 1.35 |
| | 2007 | 3,078.86 | 16.36 | | |
| | 2008 | 3,339.34 | 9.73 | | |
| | 2009 | 2,530.31 | 0.00 | | |
| | 2010 | 2,680.68 | 8.80 | | |
| | 2011 | 1,639.44 | 0.00 | | |
| | 2012 | 1,931.28 | 0.44 | | |
| | 2013 | 2,185.97 | 0.38 | | |
| | 2014 | 1,885.44 | 0.00 | | |

| Water-Discharge Stations and Site No | Years | Max 10-daily Discharge (Cumec) | Average River Bankline Shifting Rate (m) | Soil Type / Bank Material | Sinuosity Ratio |
|---|---|---|---|---|---|
| | 2015 | 950.35 | 64.04 | | |
| | 2016 | 1038.76 | 27.16 | | |
| | 2017 | 1313.13 | 1.11 | | |
| | 2018 | 1209.57 | 8.32 | | |
| | 2019 | 1457.33 | 3.62 | | |

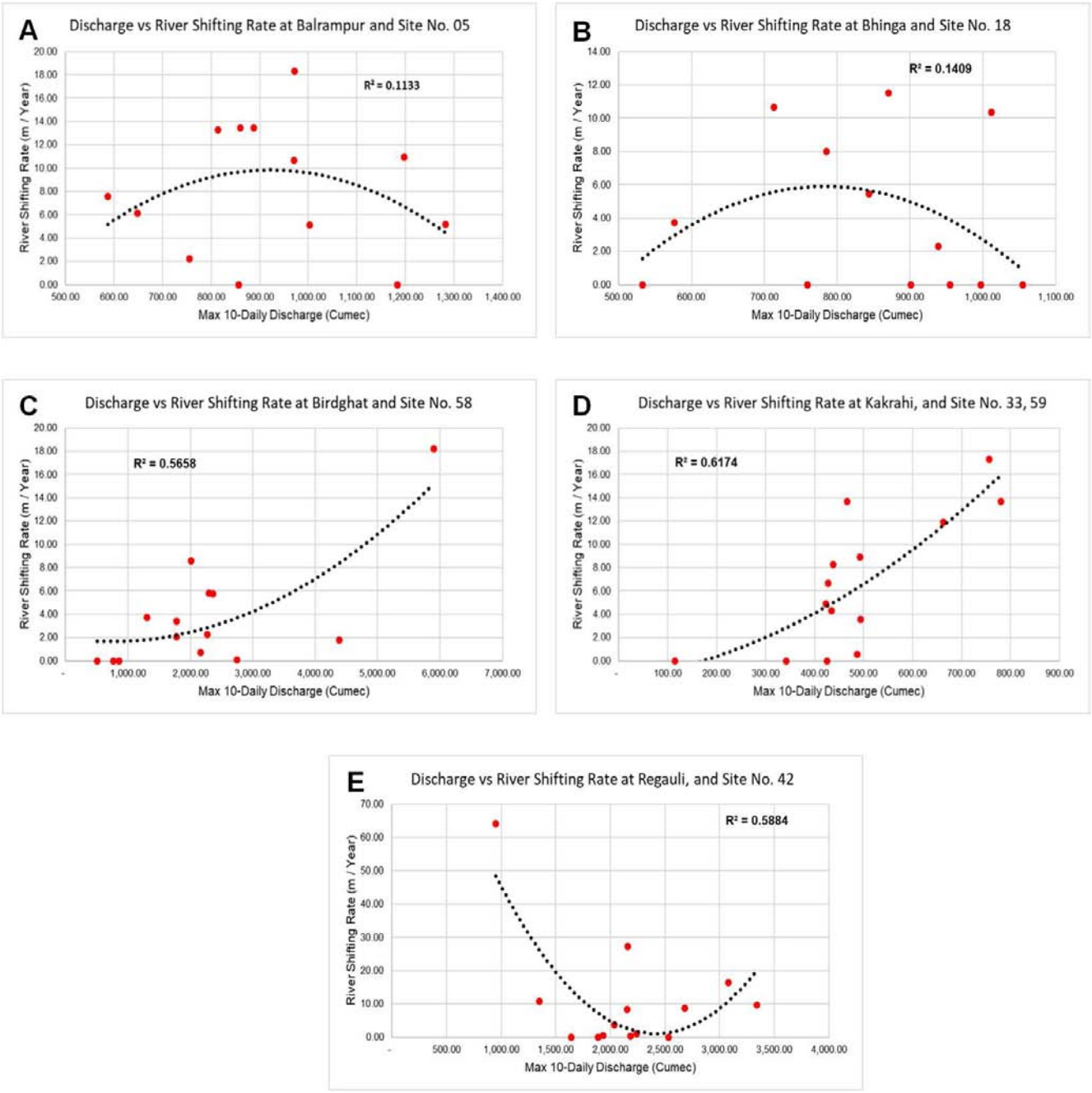


**Figure 14.** Discharge vs River Bankline Shifting Rate at 5 Gauging Sites i.e. Birdghat, Balrampur, Kakrahi, Regauli, and Bhinga of the Rapti River System.

We have attempted a relationship between discharge and river bankline shifting rate at the vulnerable sites closest to gauge stations with available data, however there was no direct correlation between these parameters. We related the average rates of river bankline shifting to the five discharge variables from Table 8, and these are shown in Figure 14. Poor correlations of $R^2 = 0.1133$ and $R^2 = 0.1409$, exist for gauge stations Balrampur (Site No. 5) and Bhinga (Site No. 18), respectively in regard to the influence of 10-daily max discharge and average river bankline shifting rate. Some generalized trends, appropriate to the scale at which the variables were measured, are apparent in Figure 14 (C, D, E).

The relationship between river shifting rate and 10-daily max discharge are correlated at Birdghat ($R^2$ = 0.5658) (Site No. 58), Kakrahi ($R^2$ = 0.6174) (Site No. 33), and Regauli ($R^2$ = 0.5884) (Site No. 42). From these values we suggest the 10-daily max discharge have the greatest effect on rates of lateral river bankline shifting. It is expected that river bank erosion and therefore river bankline shifting rates to be greater when discharge is equal to or greater than 1.5 to 2-year flood return period i.e. bank-full width.

### 6.4. Model Capability for Predicting Channel Development / Abandonment

Abandoned channels are those channels left behind as meandering rivers migrate over the floodplains. River channel development in natural condition is usually a long process unless there is a huge flood event in a particular year in which case new channel may develop suddenly. This model is capable of predicting gradual annual changes in bankline resulting in channel development and abandonment in a long time. The model is not capable of predicting new channel development that happened suddenly due to huge flood in a year.

### 6.5. Measures for Protection from Erosion in the Morphologically Active Areas

(i). Construction of embankments in the reaches which are prone to erosion and flooding.

(ii). Construction of spurs to divert flow from the river bank and embankments. Generally, spurs are used to divert river flow away from the critical zones of the bank to protect from erosion.

(iii). Installation of submerged vanes to protect the embankment and river bank from under-cutting and move the thalweg away from the embankment and river bank. Submerged vanes are a measure for sediment management in alluvial rivers. The structure consists of a system of vertical flow training vanes mounted on the channel bed with an angle to the flow ranging from 10° to 40°.

(iv). Use of revetment of proper erosion-resistant material that covers the erodible areas of the river bank. It protects the riverbank against wave and current induced loads. The cover layer of the revetment resists the impacts of current and wave. Generally, the construction materials of revetments are cement concrete blocks, boulders, and open asphalt concrete.

(v). Pitching by geo-textile bags in the vulnerable river banks/embankments. Geotextile bags provide an economic option for erosion control due to the use of locally available resources (material and labour).

## 7. Conclusion

This study aimed at understanding the morphological changes and predicting short-term river bankline shifting in the Rapti river system, India using satellite imageries and ARIMA model. Multi-temporal Landsat satellite imageries for 14 years (2006-2019) were used to measure the lateral river bankline shifting in 105 identified vulnerable sites.

Many vulnerable sites in Rapti river system that we visited need urgent attention for flood and erosion control as those areas are not equipped with proper embankments and other river training structures. Erosion is intensive in those sites and lives of human and livestock as well as land and properties are at risk. The bankline migration of Rapti river and its tributaries is rampant and urgent attention is called for. The measures taken to protect the area from flood and erosion are by and large not adequate. Some of the important embankments were constructed long back and these have a huge risk to the people and their properties in case of a breach. Embankments, spurs, studs, concrete porcupines, cutters, bamboo crates, polybags filled by river bank material, etc. are used at various vulnerable sites, but at many of the sites visited during field verification, these are eroded away or damaged by the flood water. Additional protection is required to protect the actively eroding river bankline and embankments.

These empirical and forecast models have been used to predict the morphological changes of the vulnerable sites in the near-future. Though indicative, these forecasts will aid in river management and training activities and early warning against erosion risk. To more accurately model river bankline shifting against measurement it is suggested to use the high-resolution satellite images i.e. QuickBird, GeoEye, WorldView with at-least 50 cm spatial resolution.

## Acknowledgements

Authors are grateful to the MD, DHI (India) Water & Environment Pvt Ltd, New Delhi INDIA for providing the necessary facilities to carry out this work.

## References

[1] Nanson GC and Knighton A. (1996). Anabranching rivers - their cause, character and classification. *Earth Surface Processes and Landforms. Vol. 21, pp. 217-239.*

[2] Mount NJ Tate NJ, Sarker MH and Thorne CR. (2013). Evolutionary, multi-scale analysis of riverbank line retreat using continuous wavelet transforms - Jamuna river, Bangladesh. *Geomorphology. Vol. 183, pp. 82-95.*

[3] Midha N and Mathur PK. (2014). Channel characteristics and planform dynamics in the Indian Terai, Sharda river. *Environmental Management. Vol. 53, pp. 120-134. https://doi.org/10.1007/s00267-013-0196-4.*

[4] Buffington JM. (2012). Changes in channel morphology over human time scales, gravel bed rivers - processes, tools, environments. *In: Michael Church, Pascale M. Biron and Andre' G. Roy, first ed. John Wiley & Sons, Ltd. pp. 435-465.*

[5] Sarma JN. (2005). Fluvial process and morphology of the Brahmaputra river in Assam, India. *Geomorphology. Vol. 70, pp. 226-256. https://doi.org/10.1016/j.geomorph.2005.02.007.*

[6] Sarker MH, Thorne CR, Akhtar MN and Ferdous MR. (2014). Morpho-dynamics of the Brahmaputra-Jamuna river, Bangladesh. *Geomorphology. Vol. 215, pp. 45-59. https://doi.org/10.1016/j.geomorph.2013.07.025.*

[7] Islam ARMT. (2016). Assessment of fluvial channel dynamics of Padma river in north-western Bangladesh. *Universal Journal of Geoscience. Vol. 4, pp. 41-49. https://doi.org/10.13189/ujg.2016.040204.*

[8] Friend PF and Sinha R. (1993). Braiding and meandering parameters. *Geological Society of London, Special Publication. Vol. 75, pp. 105-111.*

[9] Graf WL. (2000). Locational probability for a dammed, urbanizing stream - salt river, Arizona, USA. *Environmental Management. Vol. 25, pp. 321-335. https://doi.org/10.1007/s002679910025.*

[10] Pareta K, Jakobsen F and Joshi M. (2019). Morphological Characteristics and Vulnerability Assessment of Alaknanda, Bhagirathi, Mandakini and Kali Rivers, Uttarakhand (India). *American Journal of Geophysics, Geochemistry and Geosystems. Vol. 5 (2), pp. 49-68.*

[11] Pourbakhshian S and Pouraminian M. (2015). Stochastic modeling to prediction of river morphological changes stochastic modeling to prediction of river morphological changes. *Indian Journal of Science and Technology. Vol. 8 (11), pp. 1-10.*

[12] Ziliani L and Surian N. (2012). Modelling and prediction of channel morphology evolution in a large braided river (Tagliamento River, Italy). *In: EGU General Assembly Conference Abstracts. pp. 9784.*

[13] Keady DM and Priest MS. (1977). The downstream migration rate of river meandering patterns. *In: 12th Mississippi Water Resources Conference, Jackson, Mississippi. pp. 29-34.*

[14] Hooke JM. (1980). Magnitude and distribution of rates of river bank erosion. *Earth Surface Processes and Landforms. Vol. 5 (2), pp. 143-157.*

[15] Brice JC. (1982). Stream channel stability assessment. *Federal Highway Administration Report FHWA/RD-82/021, Washington, D. C. Vol. 41.*

[16] Nanson GC and Hickin EJ. (1983). Channel migration and incision on the Beatton river. *Journal Hydraulic Engineering, ASCE. Vol. 109 (3), pp. 327-337.*

[17] Blondeaux P and Seminara G. (1985). A unified Bar-Bend theory of river meanders. *Journal of Fluid Mechanics. Vol. 157, pp. 449-470.*

[18] Ikeda S, Parker G and Sawi K. (1981). Bend theory of river meanders, I-linear development. *Journal of Fluid Mechanics. Vol. 112, pp. 363-377.*

[19] Pizzuto JE. (1990). Numerical simulation of Gravel river widening. *Water Resources Research. Vol. 26 (9), pp. 1971-1980.*

[20] Mosselman E. (1998). Morphological modelling of rivers with erodible banks. *Hydrological Processes. Vol. 12 (8), pp. 1357-1370.*

[21] Sarker M, Kamal M and Hassan K. (1999). The morphological changes of a distributary of the Ganges in response to the declining flow using remote sensing. *In: 20th Asian Conference on Remote Sensing. Vol. 1, pp. 1-10.*

[22] Clark J and Wilcock P. (2000). Effects of land-use change on channel morphology in north-eastern Puerto Rico. *Geological Society of America Bulletin. Vol. 112, pp. 1763-1777.*

[23] Duan JG, Wang SSY and Jia Y. (2001). The applications of the enhanced CCHE2D model to study the alluvial channel migration processes. *Journal of Hydraulic Research. Vol. 39 (5), pp. 469-480.*

[24] Duan JG and Julien PY. (2005). Numerical simulation of the inception of channel meandering. *Earth Surface Processes and Landforms. Vol. 30 (9), pp. 1093-1110.*

[25] Duan JG. (2005). Analytical approach to calculate rate of bank erosion. *Journal of Hydraulic Engineering. Vol. 131 (11), pp. 980-990.*

[26] Darby SE, Alabyan AM and Wiel MJ. (2002). Numerical simulation of bank erosion and channel migration in meandering rivers. *Water Resources Research. Vol. 38 (9), pp. 21-221.*

[27] Lagasse PF, Spitz WJ and Zevenbergen LW. (2003). A methodology for ArcView tools for predicting channel migration. *ESRI, User Conference Proceedings, San Diego, California.*

[28] Abad J and Garcia MH. (2004). Conceptual and mathematical model for evolution of meandering rivers in naturalization processes. *In: World Water and Environmental Resources Congress: Critical Transitions in Water and Environmental Resources Management, Salt Lake City, Utah. pp. 2048-2057.*

[29] Merwade V, David M and Hodges B. (2005). Geospatial representation of river channels. *Journal of Hydrologic Engineering. Vol. 10.*

[30] Wang SSY and Wu W. (2006). Formulas for sediment porosity and settling velocity. *Journal Hydraulic Engineering. Vol. 132 (8), pp. 858-862.*

[31] Larsen EW and Girvetz EH. (2007). Landscape level planning in alluvial riparian floodplain ecosystems using geomorphic modeling to avoid conflicts between human infrastructure and habitat conservation. *Landscape and Urban Planning. Vol. 81, pp. 354-373.*

[32] Kummu M, Lu XX, Rasphone A, Sarkkula J and Kopone, J. (2008). Riverbank changes along the Mekong river - remote sensing detection in the vientiane - Nong Khai area. *Quaternary International. Vol. 186, pp. 100-112.*

[33] Rana NK, Kumar R and Kumar D. (2009). Nature of channel shifting of a foothills-fed river in the alluvial Settings - A case study of Rapti river. *Geomorphology. pp. 1-21.*

[34] Langbein WB and Leopold LB. (1966). River meanders theory of minimum variance. *Geological Survey Professional Paper 442-H, United States Government Printing Office, Washington.*

[35] Carvalho OA, Guimaraes RF, Santos NBF, Martins ES, Gomes RAT and Shimabukuro YE. (2010). Analysis of channel morphology of Sao Francisco river using remote sensing data. *International Journal of Remote Sensing. Vol. 31 (8), pp. 1981-1994.*

[36] Krapesch G, Hauer C and Habersack H. (2011). Scale orientated analysis of river width changes due to extreme flood hazards. *Natural Hazards and Earth System Sciences. Vol. 11, pp. 2137-2147.*

[37] Sarkar A, Garg RD and Sharma N. (2012). RS-GIS based assessment of river dynamics of Brahmaputra river in India. *Journal of Water Resource and Protection. Vol. 4, pp. 63-72. https://doi.org/10.4236/jwarp.2012.42008.*

[38] Thian YG and Baki ABM. (2013). Assessing morphological changes of the Ganges river using satellite images. *Quaternary International. Vol. 304, pp. 142-155. https://doi.org/10.1016/j.quaint.2013.03.028.*

[39] Yang S, Milliman JD, Xu KH, Deng B, Zhang XY and Luo XX. (2014). Downstream sedimentary and geomorphic impacts of the Three Gorges dam on the Yangtze river. *Earth-Science Reviews. pp. 138.*

[40] Reza AI and Reza MA. (2016). Assessment of fluvial channel dynamics of Padma river in north-western Bangladesh. *Universal Journal of Geoscience. Vol. 4, pp. 41-49.*

[41] Mallick S. (2016). Identification of fluvio-geomorphological changes and bank line shifting of river Bhagirathi-Hugli using remote sensing technique in and around of Mayapur Nabadwip Area, West Bengal. *International Journal of Scientific Research. Vol. 5, pp. 1130-1134.*

[42] Bhuayan MABS and Yorozuya A. (2016). Prediction of morphological changes in Jamuna river near Bahadurabad area. *International Centre for Water Hazard and Risk Management (ICHARM), PWRI, Japan. Synopses.*

[43] Nabi MR, Rashid MS and Hossain MI. (2016). Historical bankline shifting since 1760s - a GIS and remote sensing-based case study of Meghna river plate of Rennell's Atlas. *International Journal of Scientific and Research Publications. Vol. 6 (12), pp. 473-483.*

[44] Khan MA and Mostafa M. (2016). An approach to predict the yearly bank erosion rates of Jamuna river - an application of the correlation of bank shear stress and river discharge. *International Journal of Engineering Development and Research. Vol. 4 (2), pp. 1180-1185.*

[45] Jia Y and Scott S. (2017). Simulation of sediment transport and channel morphology change in large river systems. *US-China Workshop on Advanced Computational Modelling in Hydro-Science and Engineering. pp. 1-11.*

[46] Rahman M and Islam M. (2017). Bank erosion pattern analysis by delineation of course migration of the Padma river at Harirampur Upazila using satellite images and GIS. Part II. *Journal of Geology & Geophysics. Vol. 6, pp. 2-7.*

[47] Lai YG. (2017). Modeling stream bank erosion: practical stream results and future needs. *Water. Vol. 9 (12), pp. 950.*

[48] Lant JG and Boldt JA. (2018). River meander modeling of the Wabash river near the Interstate 64 bridge near Grayville, Illinois. *U.S. Geological Survey Scientific Investigations Report, 2017-5117. pp. 12. https://doi.org/10.3133/sir20175117.*

[49] Spada D, Molinari P, Bertoldi W, Vitti A and Zolezzi G. (2018). Multi-temporal image analysis for fluvial morphological characterization with application to Albanian rivers. *International Journal of Geo-Information. Vol. 7 (314), pp. 1-21.*

[50] Akhter SE, Islam KU, Islam ST, Reza MA, Chu R and Shuanghe R. (2019). Predicting spatiotemporal changes of channel morphology in the reach of Teesta river, Bangladesh using GIS and ARIMA modeling. *Quaternary International. Vol. 513, pp. 80-94.*

[51] Pal R and Pani P. (2019). Remote sensing and GIS-based analysis of evolving planform morphology of the middle-lower part of the Ganga river, India. *The Egyptian Journal of Remote Sensing and Space Science. Vol. 22 (1), pp. 1-10.*

[52] Sylvester Z, Durkin P and Covault JA. (2019). High curvatures drive river meandering. *Geology, Vol. 47, pp. 1-4.*

[53] Mohindra R, Prakash B and Prasad J. (1992). Historical geomorphology and pedology of the Gandak megafan, middle gangetic plains, India. *Earth Surface Process and Landforms. Vol. 17, pp. 643-662. https://doi.org/10.1002/esp.3290170702.*

[54] Box GEP and Jenkins GM. (1970). Time series analysis, forecasting and control. *Holden-Day, San Francisco, CA.*

[55] Zhang GP. (2003). Time series forecasting using a hybrid ARIMA and neural network model. *Neurocomputing. Vol. 50, pp. 159-175.*

[56] Lee J. (2000). Univariate time series modeling and forecasting (Box-Jenkins Method). *Econ. 413, Lecture 4.*

[57] Makridakis S and Hiban M. (1983). ARMA models and the Box Jenkins methodology. *Insead, Boulevard de Constance, Fontainebleau 77305 Cedex, France. https://autobox.com/makridakis.pdf*

[58] Biswajit N, Sultana N and Paul A. (2013). Trends analysis of river bank erosion at Chandpur, Bangladesh: A remote sensing and GIS approach. *International Journal of Geometrics and Geosciences. Vol. 3 (4), pp. 454-464.*

[59] Pareta K. (2013). Geomorphology and Hydrogeology: Applications and Techniques using Remote Sensing and GIS. *LAP Lambert Academic Publishing, Germany. pp. 1-413.*

[60] Esther CE. (2013). Numerical modeling of river migration incorporating erosional and depositional bank processes. *PhD thesis, Department of Civil and Environmental Engineering, University of Illinois Urbana-Champaign.*

[61] Esther CE, Matthew J, Czapiga E, Yasuyuki SJ, Sun IT and Parker G. (2014). Coevolution of width and sinuosity in meandering rivers. *Journal of Fluid Mechanics. Vol. 760, pp. 127-174.*

[62] International Fact-Finding Mission. (2005). Report on cases of violations of the right to food in Uttar Pradesh, India. *November 2004, Oslo (FIAN Norway).*

[63] Andrle R. (1994). The angle measure technique: a new method for characterizing the complexity of geomorphic lines. *Mathematical Geology. Vol. 26, pp. 83-97.*

[64] Andrle R. (1996). Complexity and scale in geomorphology: statistical self-similarity vs. characteristic scales. *Mathematical Geology. Vol. 28, pp. 275-293.*

[65] Charlton R. (2008). Fundamentals of fluvial geomorphology. *London, 234 Routledge. pp. 80.*

[66] Pareta K and Pareta U. (2019). Hydro-geomorphological mapping of Rapti river basin (India) using ALOS PALSAR (DEM), GRACE/GLDAS and Landsat-8 remote sensing data. *American Journal of Geophysics, Geochemistry and Geosystems. Vol. (5) 3, pp. 104-118.*

[67] Dey S. (2014). Fluvial Hydrodynamics, Hydrodynamic and Sediment Transport Phenomena. *Geo-Planet, Earth and Planetary Sciences, Springer-Verlag Berlin Heidelberg. pp. 529-562.*

[68] Pareta K and Pareta U. (2017). Geomorphological analysis and hydrological potential zone of Baira river watershed, Churah in Chamba district of Himachal Pradesh, India. *Indonesian Journal of Science and Technology. Vol. 2 (1), pp. 26-49.*

[69] Pareta K and Pareta U. (2012). Quantitative geomorphological analysis of a watershed of Ravi river basin, H. P. India. *International Journal of Remote Sensing & GIS. Vol. 1 (1), pp. 47-62.*